ALTERNATIVE APPROACH TO POWER LINE COMMUNICATION (PLC) CHANNEL MODELLING AND MULTIPATH CHARACTERIZATION

by

Steven Omondi Awino

Dissertation submitted in fulfilment of the requirement for the degree
MASTER OF SCIENCE IN ENGINEERING: ELECTRONIC ENGINEERING
in the
School of Engineering

UNIVERSITY OF KWAZULU-NATAL

Supervisor: Prof. Thomas Joachim Odhiambo Afullo

March 2016

As the candidate's supervisor, I have approved this dissertation for submission.

Signed . . . . Date . . . .

Name: Prof. Thomas J. O. Afullo

Declaration 1 - Plagiarism

I, **Steven Omondi Awino**, declare that

1. The research reported in this dissertation, except where otherwise indicated, is my original research.

2. This dissertation has not been submitted for any degree or examination at any other university.

3. This dissertation does not contain other persons' data, pictures, graphs or other information, unless specifically acknowledged as being sourced from other persons.

4. This dissertation does not contain other persons' writing, unless specifically acknowledged as being sourced from other researchers. Where other written sources have been quoted, then:

   (a) Their words have been re-written but the general information attributed to them has been referenced

   (b) Where their exact words have been used, then their writing has been placed in italics and inside quotation marks, and referenced.

5. This dissertation does not contain text, graphics or tables copied and pasted from the Internet, unless specifically acknowledged, and the source being detailed in the dissertation and in the References sections.

Signed ....Date ....

Declaration 2 - Publications

Details of publications directly related to this Dissertation including their overlapping Chapters:

1. **Steven O. Awino** and Thomas J. O. Afullo, "Power Line Communication Channel Modelling Using Parallel Resonant Circuits Approach," in *Proceedings of SATNAC*, Western Cape, South Africa, 6-9 September, 2015.

2. **Steven O. Awino** and Thomas J. O. Afullo, "Measurements and Multipath Characterization of Power Line Communication Channel," *Proceedings of SAUPEC*, Vaal University of Technology, South Africa, 26-28 January, 2016.

In the first paper, results of low-voltage Power Line Communication (PLC) channel transfer function in the frequency range of 1-30 MHz are presented. The power line network is studied under the extreme case with short circuited branch termination. A Parallel Resonant Circuit (PRC) channel model is then proposed. Validation of the simulated model is then done through measurements on a test bed for different network configurations under study. Transverse Electromagnetic (TEM) transmission line resonant circuit theory approach is employed to optimize the obtained parameters of the model. The PRC model results are then compared to the SRC model and found to match very well and therefore the model is considered appropriate for the characterization of the power line network channel.

The second paper presents measurement and analysis results of the in-door low-voltage Power Line Communication (PLC) network time variant and multipath characteristics under different unknown network topologies in the frequency band of 1-30 MHz. Based on the measurement results, a conventional method of estimating the Root Mean Square (RMS) delay spread and other delay parameters from the average impulse response delay profiles is used to extract the multipath characteristic parameters and associated coherence bandwidths for each network. From the results obtained, the RMS delay spread is observed to increase with the complexity of the network topology, which leads to a reduction in the coherence bandwidths. The results obtained are also compared to models of similar approach and found to be comparable.

Signed ....Date ....

Acknowledgements

Abstract

Modelling and characterization of the Power Line Communication (PLC) channel is an active research area. The research mainly focuses on ways of fully exploiting the existing and massive power line network for communications. In order to exploit the PLC channel for effective communication solutions, physical properties of the PLC channel need to be studied, especially for high bandwidth signals. In this dissertation, extensive simulations and measurement campaigns for the channel transfer characteristics are carried out at the University of KwaZulu-Natal in selected offices, laboratories and workshops within the Department of Electrical, Electronic and Computer Engineering.

Firstly, we employ the Parallel Resonant Circuit (PRC) approach to model the power line channel in chapter 4, which is based on two-wire transmission line theory. The model is developed, simulated and measurements done for validation in the PLC laboratory for different network topologies in the frequency domain. From the results, it is found that the PRC model produces similar results to the Series Resonant Circuit (SRC) model, and hence the model is considered for PLC channel modelling and characterization.

Secondly, due to the time variant nature of the power line network, this study also presents the multipath characteristics of the power line communication (PLC) channel in chapter 5. We analyse the effects of the network characteristics on the received signal and derive the multipath characteristics of the PLC channel from measured channel transfer functions by evaluating the channel impulse responses (CIR). The results obtained are compared with results from other parts of the world employing similar approach based on the Root Mean Square (RMS) delay spread and are found to be comparable. Based on the CIR and extracted multipath characteristics, further research in PLC and related topics shall be inspired.

Contents

List of Figures

List of Tables

Chapter 1

INTRODUCTION TO POWER LINE COMMUNICATION

1.1 Power Line Communication (PLC) Overview

Power line communication (PLC) is the transmission of high frequency modulated carrier signal on conductors that are used for electrical power distribution. It involves data, voice and video transfer through electrical power networks. Electrical power networks have been used for ages for internal communication of electrical utilities and for the realization of remote measuring and control tasks [11], [12], [13], [14], [15]. But due to increased necessity for new telecommunications services and technologies with increased bandwidth capacities, network providers are seeking to find cost effective solutions to their infrastructural requirements. An alternative solution for the realization of these networks is offered by the PLC technology [7]. The main idea in realization of PLC is the reduction in the operational costs and expenditure in the realization of new telecommunication network [12], [13], [15], [16]. Economically, high-voltage, medium-voltage, and low-voltage electrical power supply networks offer the cheapest medium for PLC since these electrical networks are already installed [14–16]. In addition, the electrical networks are the most reliable for communication carrier signals because of their sturdy construction that allows them to withstand natural hazards [13, 14]. In fact the power lines are the most reliable for carrier information than for power transmission, because most faults that make a line incapable of carrying power still leave sufficient insulation for the relatively low carrier voltage to provide a reliable carrier operation [13].

The application and use of electrical power supply networks in the field of Telecommunication has been in existence for a long time [13], [17], [18], [19], [20], [21], [22]. The first Carrier Frequency Systems (CFS) were operated in high-voltage electrical power supply networks that spanned distances over 500 Km using 10-W signal transmission power [13, 15] for internal communication of electrical utilities and realization of remote measuring and control tasks. Also, communication over medium-voltage and low-voltage electrical power supply networks has been realized through application of Ripple Carrier Signalling (RCS) systems for the realization of load management in electrical supply networks and systems [12, 14, 15].

In-home (popularly called in-door) electrical power networks have been used for the realization of numerous automation and control services [15, 22]. In-door PLC system has made it possible for the management of various electrical equipment within buildings and

private homes from a central control point without the installation of extra communication networks [13, 15, 22]. Other uses of in-door PLC systems include security surveillance, monitoring of heating devices, and light control, among other uses [22, 23].

PLC exploits widely available electrical power supply networks for communications. However, no universal model exists to define and characterize the PLC channel. This is because electrical power networks present unpredictable and harsh conditions for data transmission. Furthermore, the PLC channel is characterized by frequency dependent attenuation, ever-varying channel impedance, and multipath fading besides impulsive noise conditions. In an attempt to address these problems, various models and modulation schemes have been presented by various researchers as mitigation measures but with some success. For this reason, this work is directed to the study of the electrical power line channel and to give a set of results that could be considered for the design and implementation of broadband PLC systems. This is done through modelling and multipath characterization of the power line network.

1.1.1 Power Supply Networks and Characteristics

The electrical power supply network consist of three different network levels as shown in Figure 1.1 that are available for the realization of PLC [14, 24, 25]:

- High-voltage network (110-330 KV): These networks connect the power generating stations to large supply areas. They have very long hop lengths to cover the equally long distances, allowing for even power transmission across countries. In addition, these networks are implemented through overhead electrical cables.

- Medium-voltage network (10-30 KV): These networks connect larger regions, cities and commercial customers. They cover shorter distances than the high-voltage networks and are implemented through overhead and underground electrical cables.

- Low-voltage network (230/400 V): These networks supply the end users and customers. Their line lengths are usually up to a few hundred meters. Low-voltage networks are realized by both overhead and underground cables. They are mainly used for in-door PLC communication.
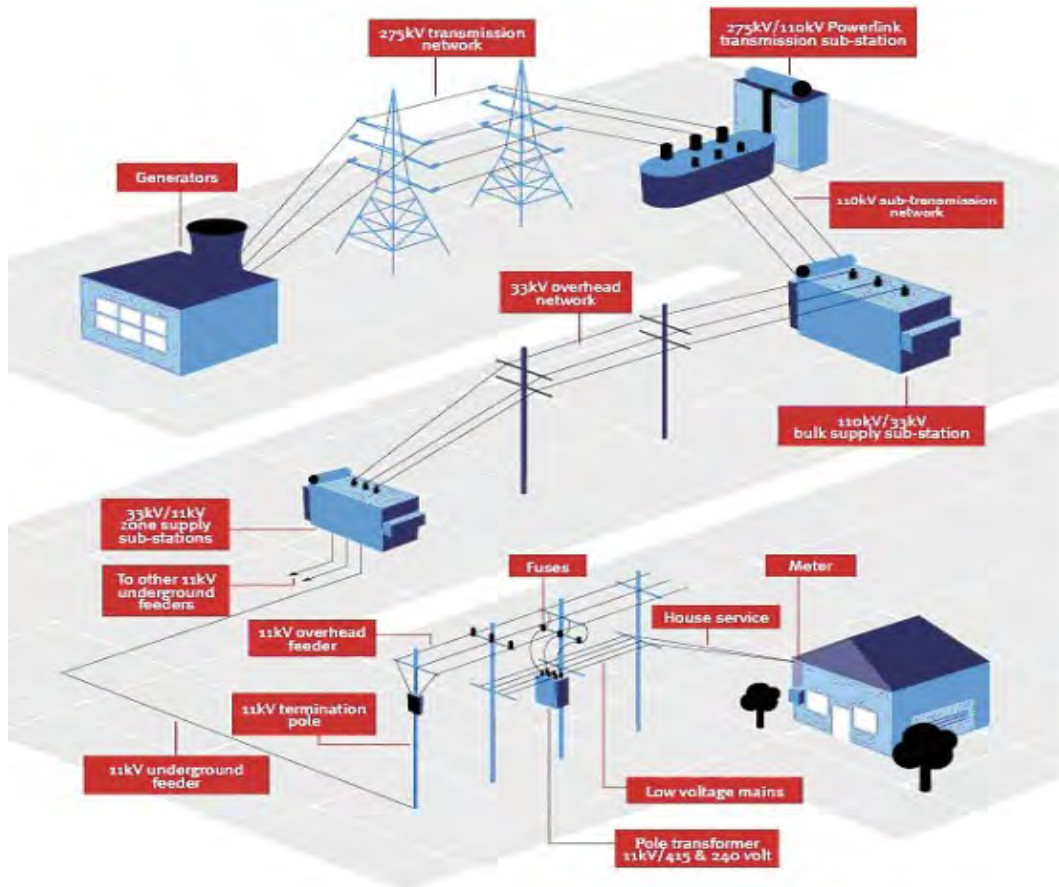
Figure 1.1: Electrical power supply network [from *https://dews.qld.gov.au Sept. 2015*]

The three different levels of electrical power supply networks have very unique characteristics. In summary, the principle characteristics of the electrical power line network are:

- Ever changing line impedance: This factor is mainly influenced by the characteristic impedance of the power line cables, the topology of the network and the nature of the connected electrical loads. Based on several measurement campaigns by PLC researchers, the impedance of the electrical power line network has been confirmed to be ever varying with frequency and time [11], [26], [27], [28]. Because of this complex impedance, achievement of impedance matching at terminal access points to the power line network has not been fully realized since the electrical power network can never be put into passive conditions.

- Attenuation and propagation loss: In high frequency communication, cable losses and the increasing length of the transmission cables result in attenuation and propagation losses dependant on the frequency of transmission [11], [23], [29], [30], [31]. This characteristic is common in PLC system due to the high frequencies used for signal transmission.

- Interference: The injection of PLC signals into the power lines result in the radiation

3

of electromagnetic fields in the environment. This makes the power lines to act like antennas from the electromagnetic point of view. This interference has a broadband spectra in the frequency domain [14] and thus cause interference in PLC system.

- Multiple impedance discontinuities: The electrical power line network is an interconnection of numerous short length transmission lines supplying electrical energy to different points [26, 30]. Because of this, there exist several branching and terminal points that make this network to be a network of multiple impedance discontinuities.

- Impulsive noise: The electrical power line network is characterized by an 'ON' and 'OFF' connection of electrical equipment into and out of the network. This results in high amplitude impulses of short durations ranging from some microseconds up to a few milliseconds generated into the channel [20], [21], [28], [32], [33], [34].

1.1.2 In-door PLC Network Structure

The in-door electrical power supply networks are at the low-voltage network level. In this network level, the customers own the electrical installations, while the outdoor network belong to the electrical supply utilities [35]. From Figure 1.2, these installations are normally connected to the grid through the meter-unit, (MU) and are easily optimized for in-door or in-home PLC by installing a PLC access point, (AP) besides their basic function of supplying electrical power to electrical and electronic loads.

Due to the direct connection of the low-voltage electrical power supply network to a large number of customers, the application of PLC technology in this network seems to have a prospective regarding the number of connected clients. In addition, the low-voltage network covers a small distance from the transformer unit to the customers thereby allowing for the realization of the so called 'last mile' communication in the telecommunication access area [7, 13, 14].
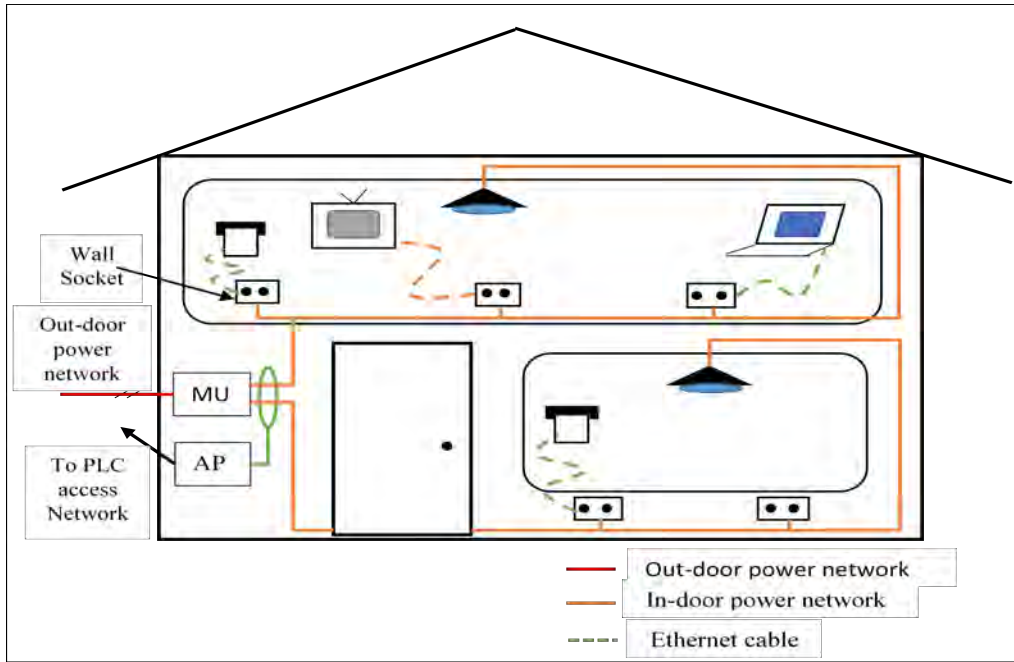
Figure 1.2: Typical in-door PLC network structure

A simple PLC system consists of the following three distinct parts as in Figure 1.3. A high frequency signal is injected into the power line network from the transmitter through the couplers and propagates to the receiver. As this signal propagates through the power line channel, it is subject to distortion from noise [20], [21], [28], [32], [33] within the channel itself and from the terminal points, attenuation and multipath fading due to the ever changing characteristics of the channel. These factors are a major impairment and drawback to PLC systems. The couplers provide a means of connecting terminal modems and communication equipment to the power line network, blocking the 230 V, 50 Hz frequency electrical energy as well as providing a means of equipment protection from the mains.
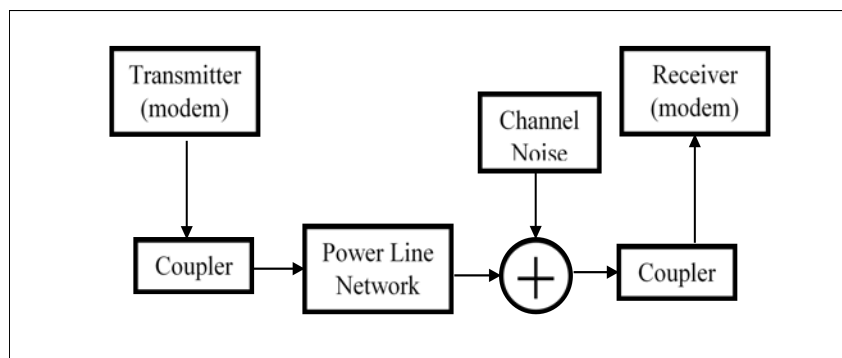
Figure 1.3: Block diagram of a PLC system

1.1.3 PLC System Impairments and drawbacks

It is a well-known fact that power lines were designed for electrical power distribution and transmission at high-voltages with low-frequency of 50/60 Hz [14]. So by injecting a signal of high frequency at low-voltage into the same line, the line impedance changes and becomes a varying quantity that depends on time and frequency, among others [19, 26, 36]. Therefore, power lines present very harsh conditions for transmission of carrier information signal at high frequency and low-voltage. This unique characteristic of the power lines as a channel for communication, presents the following impairments and drawbacks [14], [15], [37], [38]:

- Carrier signal undergoes attenuation due to high frequency channel losses.

- Electromagnetic wave reflections at mismatched line terminations, resulting in multipath signal propagation within the channel.

- Time and frequency varying network characteristics due to influence of capacitive and inductive loads.

- High noise level due to the 'ON' and 'OFF' switching of electrical equipment during connection and disconnections to and from the network.

- Electromagnetic interference from radio frequency channels operating within the designated PLC frequency bands.

1.1.4 PLC Standards and Regulations

Due to the wide geographical coverage of the electrical power distribution networks in different regions, different regional and international regulatory bodies have developed and adopted different standards and regulations for PLC within their regions. These regulations restrict the amount of signal bandwidth and power transmitted in power line networks. This is done in order to limit interference with other users of low frequency radio communications and prohibit further pollution of the electromagnetic spectrum.

Currently in PLC, several (different) standards exist in different countries and there is a progressive development towards a unified standard. The only reason for such numerous different standards, is due to the different laws from one country to another. In this regard therefore, we highlight the several standards that are evolving. Thorough and detailed information can be found in [7], [17], [39], [40], [41], [42], [43], [44]:

- Home-Plug Power Alliance: The Home-Plug Power Alliance is the family name for various PLC system that support networking over existing home electrical wiring.

- Institute of Electrical and Electronic Engineers (IEEE): This standard is due to IEEE broadband over power line group. The standard exists in different working groups which deal with hardware standards for PLC equipment, Electromagnetic Compatibility (EMC), among others.

- European Telecommunications Standards Institute (ETSI): This standard discusses and adopts interoperability and co-existence of the different manufactured power line equipment.

- POWERNET: This group develops and validates a 'plug and play' cognitive broadband PLC equipment.

- Universal Power-Line Association (UPA): The UPA deals with the alignment of different PLC global industry leaders in ensuring that the consumer benefits from the interoperability of the different manufactured PLC infrastructure and equipment.

- Open PLC European Research Alliance (OPERA): OPERA is a consortium composed of participants and all types of stakeholders in PLC. These stakeholders include: main utilities in Europe, the most important PLC technology providers, all universities involved in PLC research, telecom operators and engineering companies with experience in PLC.

- ITU-T G.9955 and G.9956 Recommendations: This is one of the most recent approved standards for Narrowband PLC. It defines the physical and data link layers specifications to enable cost-effective smart grid applications.

PLC operations are divided into two depending on the frequency of operation as follows:

- Narrowband PLC: This system offers a data transmission rate of up to 100 Kbps. This technology allows for the implementation of various automation and control applications besides a few voice channels. The frequency of operations is below 500 KHz. The application of Narrowband PLC has led to the realization of smart grid distribution grids over the high and medium-voltage networks [45]. Smart grid distribution supports low degree of communication and automation services.

- Broadband PLC: This system allows data transmission at rates higher than 2 Mbps, and hence suited for the implementation of data services, Internet access and telephony services. The broadband PLC technology seems to be a cost effective solution for 'last mile' communication networks. The frequency of operations is within 1 MHz to 30 MHz. However, service frequencies up to 100 MHz has been proposed to enable achievement of good quality services

In this research, we conduct our analysis and investigations within the broadband PLC frequencies of 1 MHz to 30 MHz.

1.2   Research Objectives

The objectives of this work entail the following:

- To study the characteristics of low-voltage power supply networks and compare theoretical and simulated models to measurements. This is done in the frequency domain in order to determine the influence of different network properties on the characteristics of the PLC channel.

- To compare the proposed parallel resonant circuit (PRC) model results to the existing series resonant circuit (SRC) model for different network configurations.

- To characterize the time varying and multipath characteristics of the low-voltage power supply network channel from the measured channel transfer functions. This is accomplished in conjunction with theoretical derivations of the multipath propagation parameters for different network topologies and terminal loads, as well as drawing relations for the variation in channel properties.

- To compare the mean time delay parameters obtained with previous results from the University of KwaZulu-Natal and results from other parts of the world. From the multipath characteristics in the time domain, we also draw relations for the variation of the network topology.

1.3 Methodological Approach

- Literature Review: Establishing existing theoretical basis of the study, further establishing the existing techniques to model and characterize the channel.

- Power line network simulations: Designing and analysing channel parameters through simulations to test the proposed model in the frequency domain.

- Power line network measurements: Setting up test bed networks and performing measurements to validate established channel models in the frequency domain. In addition, to measure the power line channel transfer functions under different and unknown network topologies.

- Data analysis: To extract and characterize data obtained from measurements, with a view to determining the multipath propagation delay characteristics and establishing their relations to different and unknown network topologies and load conditions.

- Comparison and validation of the results obtained with those obtained with existing models.

1.4 Significance of Study

There has been limited knowledge on signal propagation based on theoretical aspects in PLC channel. Thus, in this work, we seek to make a contribution to the ongoing research on PLC channel characterization and signal propagation. This is done through analysis and measurements of the power line channel to better the understanding and knowledge

about the channel behaviour and the multipath delay properties of the power line network channel.

1.5   Thesis Organization

The dissertation is organized as follows:

In chapter 1, we introduce the idea, standards, history and evolution of PLC systems. A review of basic and key concepts of signal transmission over low-voltage power line is presented in chapter 2. This review also entails the study of existing key contributions and efforts on PLC channel modelling and characterization of the multipath propagation characteristics of the channel.

Chapter 3 entails a detailed outline of the measurement procedures used throughout this research. In this chapter, the measuring instrument, the coupler and the test bed power line networks are presented in addition to the unknown networks.

The next two chapters, that is, chapter 4 and 5, are focused on the contributions made by the author as declared under publications. Their focus is on channel modelling in the frequency domain and multipath characterization of the channel in the time domain respectively. This dissertation is concluded by a summary of the results obtained in the two main chapters mentioned above.

Chapter 2

LITERATURE REVIEW

2.1 Introduction

PLC utilizes the existing electrical power transmission lines for data transmission. However, the power line network presents numerous challenges for data transmission due to the ever varying impedance with time and frequency resulting in multipath propagation effects, and attenuation among other drawbacks. It is for these reasons that we review the basic concepts of signal propagation through a wired transmission medium based on a two-wire transmission line model. This study is also extended to multipath propagation in the power line channel. Furthermore, key literature contributions and models in the field of PLC are reviewed with a brief introduction to the proposed models.

2.2 Transmission Line Analysis

A power line is basically a transmission line that consists of two or more parallel conductors used to connect a source to a load. In PLC, the live and neutral conductors are used for data transmission. The source in PLC, is a transmitter modem or a signal generator source transmitting information signals to the receiver modem or a measuring instrument like a network analyzer. Transmission lines are used at low frequency in electrical power distribution and at high frequency in communications. Typical transmission lines used for communications include coaxial cable, two-wire lines, fibre optic cables, among others [7, 16, 46]. In PLC, we utilize the electrical power distribution network for transmission of communication signal at low-voltages but at high frequencies. Transmission line problems are usually solved using Electromagnetic (EM) field theory and electric circuit theory which are the main theories of electrical and electronic engineering [1, 16, 47]. In this research, therefore, we employ circuit theory to analyse the power line mathematically as well as application of the basic concepts of wave propagation such as propagation constant, and reflection coefficient [1], [2], [16], [47]. In our analysis, transmission line equations and characteristic quantities are derived in order to obtain the secondary line parameters [1].

2.2.1 Transmission Line Equations

Since we are transmitting data over power transmission line, it is customary and convenient to describe a transmission line in terms of its assumed uniformly distributed primary line parameters that include: resistance per unit length R, inductance per unit length L,

conductance per unit length G, and capacitance per unit length C [1, 2, 47] as shown in Figure 2.1.
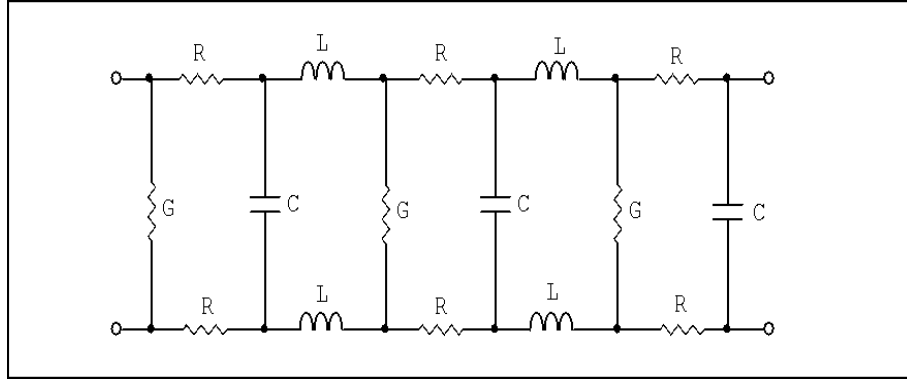
Figure 2.1: Distributed parameters of a two-wire transmission line [1]

These primary line parameters are calculated individually based on the cable electrical and dielectric structure. In this work, we employ measured and calculated primary parameters for power line transmission lines as presented in [29].

By considering an incremental portion of length of the two-wire transmission in Figure 2.1, we then proceed with an equivalent circuit for this line as in Figure 2.2 and derive the line equations [1], [2], [9], [47], assuming that the wave propagates along the $+z$ direction, from the generator to the load [1].

By applying Kirchoff's voltage law to the outer loop of the circuit in Figure 2.2, we obtain [1, 2]:

$$\frac{V(z + \Delta z, t) - V(z, t)}{\Delta z} = RI(z, t) + L\frac{\partial I(z, t)}{\partial t} \tag{2.1}$$
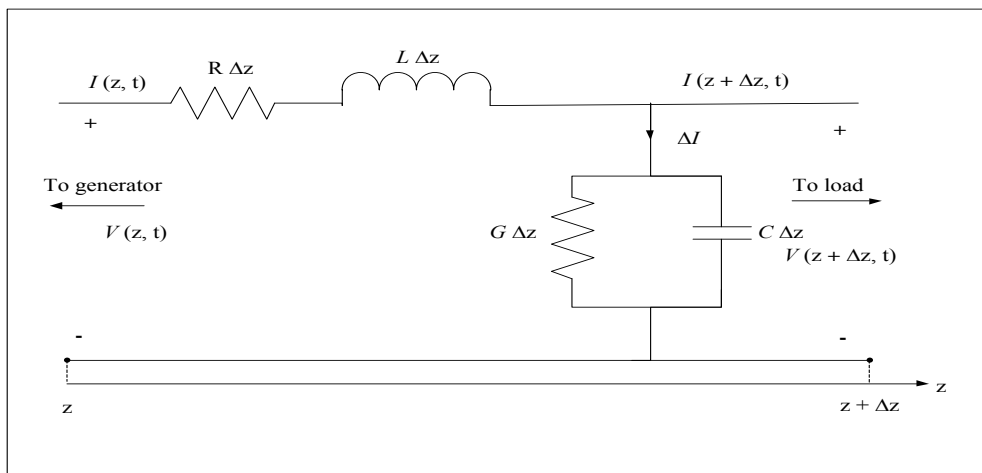
Figure 2.2: Equivalent circuit model of a differential length of a two-wire conductor transmission line [1]

Taking the limits of Equation (2.1) as $\Delta z \to 0$ leads to [1, 2]:

$$-\frac{\partial V(z,t)}{\partial z} = RI(z,t) + L\frac{\partial I(z,t)}{\partial t} \tag{2.2}$$

Similarly, applying Kirchoff's current law to the main node in Figure 2.2 gives [1, 2]:

$$\frac{I(z+\Delta z,t) - I(z,t)}{\Delta z} = GV(z+\Delta z,t) + C\frac{\partial V(z+\Delta z,t)}{\partial t} \tag{2.3}$$

As $\Delta z \to 0$, Equation (2.3) becomes:

$$-\frac{\partial I(z,t)}{\partial z} = GV(z,t) + C\frac{\partial V(z,t)}{\partial t} \tag{2.4}$$

Harmonic time dependence is assumed so that [1]:

$$V(z,t) = R_e[V_s(z)e^{j\omega t}] \tag{2.5}$$

$$I(z,t) = R_e[I_s(z)e^{j\omega t}] \tag{2.6}$$

where $V_s(z)$ and $I_s(z)$ are the phasor forms of $V(z,t)$ and $I(z,t)$ respectively. Equations (2.2) and (2.4) become:

$$-\frac{dV_s}{dz} = (R + j\omega L)I_s \tag{2.7}$$

$$-\frac{dI_s}{dz} = (G + j\omega C)V_s \tag{2.8}$$

By taking the second derivatives of equations (2.7) and (2.8), we obtain the wave propagation equations as [1, 2]:

$$\frac{d^2 V_s}{dz^2} - \gamma^2 V_s = 0 \tag{2.9}$$

$$\frac{d^2 I_s}{dz^2} - \gamma^2 I_s = 0 \tag{2.10}$$

where

$$\gamma = \alpha + j\beta = \sqrt{(R + j\omega L)(G + j\omega C)} \tag{2.11}$$

is the propagation constant (in per meter), α is the attenuation constant (in nepers per meter), and β is the phase constant (in radians per meter). The wavelength λ and wave velocity v_p are respectively, given by [1, 2]:

$$\lambda = \frac{2\pi}{\beta} \tag{2.12}$$

$$v_p = \frac{\omega}{\beta} = f\lambda \tag{2.13}$$

The travelling wave solutions to Equations (2.9) and (2.10) can be found as [1, 2]:

$$V_s(z) = V_o^+ e^{-\gamma z} + V_o^- e^{\gamma z} \tag{2.14}$$

$$I_s(z) = I_o^+ e^{-\gamma z} + I_o^- e^{\gamma z} \qquad (2.15)$$

where V_o^+, V_o^-, I_o^+, and I_o^- are the wave amplitudes. The $e^{-\gamma z}$ term represents wave propagation in the $+z$ direction and the $e^{\gamma z}$ term represents wave propagation in the $-z$ direction. Thus, the instantaneous expression for voltage is given by [1, 2]:

$$V(z, t) = R_e[V_s(z)e^{j\omega t}] \qquad (2.16)$$

$$= V_o^+ e^{-\alpha z} cos(\omega t - \beta z) + V_o^- e^{\alpha z} cos(\omega t + \beta z) \qquad (2.17)$$

To determine the characteristic impedance Z_o of the line at any point along the line, we find the ratio of positively travelling voltage wave to current wave as [1, 2]:

$$Z_o = \frac{V_o^+}{I_o^+} = -\frac{V_o^-}{I_o^-} = \frac{R + j\omega L}{\gamma} = \frac{\gamma}{G + j\omega C} = \sqrt{\frac{R + j\omega L}{G + j\omega C}} \qquad (2.18)$$

2.2.2 Terminated Transmission Line

Because the electrical power line network is a composition of short terminated transmission lines at various terminations including the load connection points (socket outlets), we thus proceed with our analysis into finding the general solutions to a lossy terminated power transmission line.

As already noted, the general solutions for current I and voltage V at a distance from the source are given by Equations (2.14) and (2.15). Let us now consider a transmission line of length l, characterized by propagation constant γ, and characteristic impedance Z_o, terminated in a load of impedance Z_L as shown in Figure 2.3.
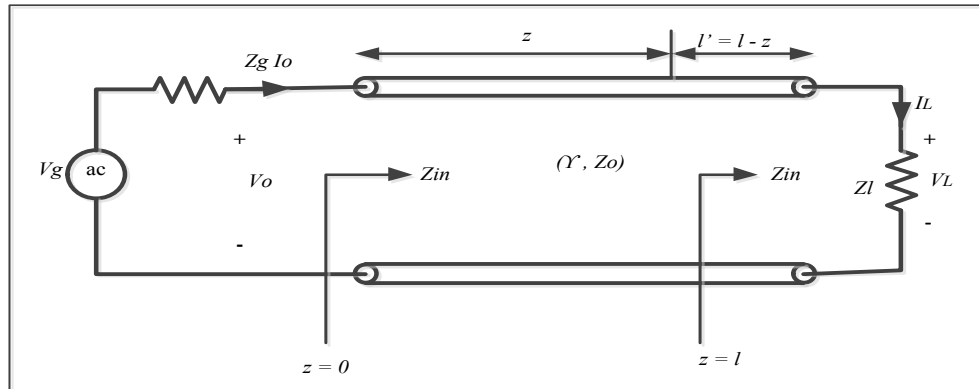
Figure 2.3: Input impedance due to a line terminated by a load [1]

To find the voltage and current in Equations (2.14) and (2.15), we incorporate Equation (2.18) and let the transmission line extend from $z = 0$ at the generator to $z = l$ at the

load, so that [1, 2]:

$$V_s(z) = V_o^+ e^{-\gamma z} + V_o^- e^{\gamma z} \tag{2.19}$$

$$I_s(z) = \frac{V_o^+}{Z_o} e^{-\gamma z} - \frac{V_o^+}{Z_o} e^{\gamma z} \tag{2.20}$$

Additionally, let the line be fed by a generator of source voltage V_g with impedance Z_g see a line with the load as an input impedance Z_{in}. Therefore, to find V_o^+, and V_o^-, we apply the terminal conditions at the input, $V_o = V(z = 0)$, and $I_o = I(z = 0)$ and substitute them into Equations (2.19) and (2.20) resulting in [1, 2]:

$$V_o^+ = \frac{1}{2}(V_o + Z_o I_o) \tag{2.21}$$

$$V_o^- = \frac{1}{2}(V_o - Z_o I_o) \tag{2.22}$$

Since the input impedance at the input terminal is Z_{in}, the input voltage V_o and the input current I_o are easily obtained from Figure 2.3 as [1]:

$$V_o = \frac{Z_{in}}{Z_{in} + Z_g} V_g, I_o = \frac{V_g}{Z_{in} + Z_g} \tag{2.23}$$

On the other hand, with these given conditions at the load, $V_L = V(z = l)$, and $I_L = I(z = l)$ and substituting into Equations (2.14) and (2.15) gives [1]:

$$V_o^+ = \frac{1}{2}(V_L + Z_o I_L)e^{\gamma l} \tag{2.24}$$

$$V_o^- = \frac{1}{2}(V_L - Z_o I_L)e^{-\gamma l} \tag{2.25}$$

To determine the input impedance $Z_{in} = V_s(z)/I_s(z)$ at any point along the line, for example at the generator, Equation (2.11) yields [1]:

$$Z_{in} = \frac{V_s(z)}{I_s(z)} = \frac{Z_o(V_o^+ + V_o^-)}{V_o^+ - V_o^-} \tag{2.26}$$

Substituting Equations (2.24) and (2.25) into (2.26) and utilizing the identities $cosh\gamma l = (e^{\gamma l} + e^{-\gamma l})/2$ and $sinh\gamma l = (e^{\gamma l} - e^{-\gamma l})/2$, we obtain [1, 2, 47]:

$$Z_{in} = Z_o \left[\frac{Z_L + Z_o tanh\gamma l}{Z_o + Z_L tanh\gamma l} \right] \tag{2.27}$$

Equation (2.27) shows that the input impedance varies periodically with the distance l from the load. We then define the voltage reflection coefficient Γ_L (at the load) for Figure 2.4 as the ratio of the voltage reflection wave to the incident wave at the load. That is [2, 47]:
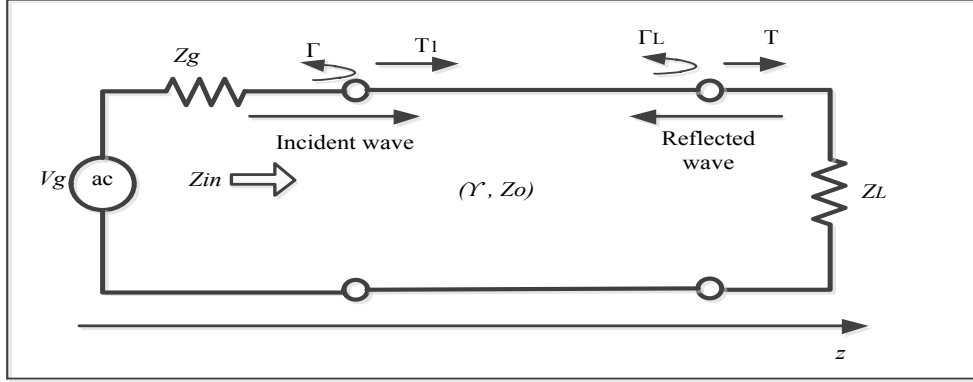
Figure 2.4: Reflections at the load [2]

$$\Gamma_L = \frac{V_o^-}{V_o^+} = \frac{Z_L - Z_o}{Z_L + Z_o} \tag{2.28}$$

As the incident signal wave propagates the channel, it suffers reflections at the load given by a transmission coefficient, T, as [2]:

$$T = 1 + \Gamma_L = 1 + \frac{Z_L - Z_o}{Z_L + Z_o} = \frac{2Z_L}{Z_L + Z_o} \tag{2.29}$$

For impedance at a branching point (node) in the power line network as shown in Figure 2.5, the associated reflection coefficient is obtained by assuming the branches to be in parallel connection with each other. Hence the total impedance of n branches on a particular node is given by [3]:
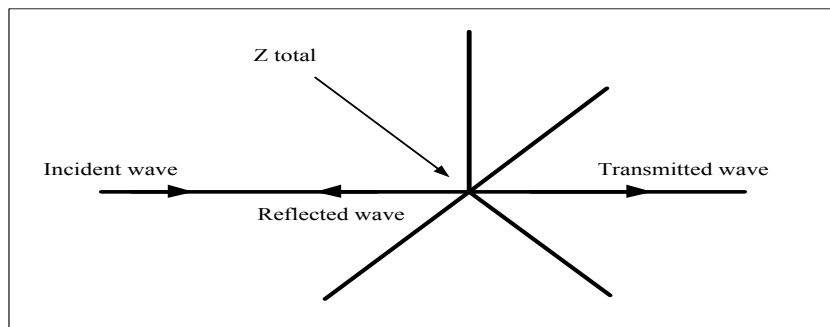
Figure 2.5: Reflections at a branching point [3]

$$Z_{total} = Z_1 // Z_2 // Z_3 // \cdots // Z_{n-1} \tag{2.30}$$

Here, n is the total number of branches extending from the branch.

Since we have confirmed that the network cables are of the same characteristic

15

impedances as presented in [29], the incidence wave will then see an impedance given by [3]:

$$Z_{total} = \frac{Z_o}{n-1}, n > 1 \tag{2.31}$$

Based on Equations (2.29) and (2.30), the reflection and transmission coefficient at the branching point are thus given as [3]:

$$\Gamma_L = \frac{Z_{total} - Z_o}{Z_{total} + Z_o} = \frac{2-n}{n} \tag{2.32}$$

$$T = \frac{2}{n} \tag{2.33}$$

2.2.3 Two-Port Network analysis of Transmission Line

The power line can also be considered as a two-port network since it has two separate ports for the input and output [48]. Based on this two-port analogy, we are thus able to characterize and relate the terminal quantities using the well-known scattering and transmission matrices. The scattering matrix relates the voltage waves incident on the ports to those reflected from the ports [2]. Because we are using a Vector Network Analyzer for our measurements, the scattering parameters are measured directly as discussed in chapter 3. Once we have obtained the scattering parameters S of the network, we can easily convert to the $ABCD$ transmission matrix [2]. Considering a two-port network in Figure 2.6, the scattering matrix links the incident waves a_1, a_2 to the outgoing waves b_1, b_2 according to the following linear equation [2, 4]:

$$\begin{bmatrix} b_1 \\ b_2 \end{bmatrix} = \begin{bmatrix} S_{11} & S_{12} \\ S_{21} & S_{22} \end{bmatrix} \begin{bmatrix} a_1 \\ a_2 \end{bmatrix} \tag{2.34}$$
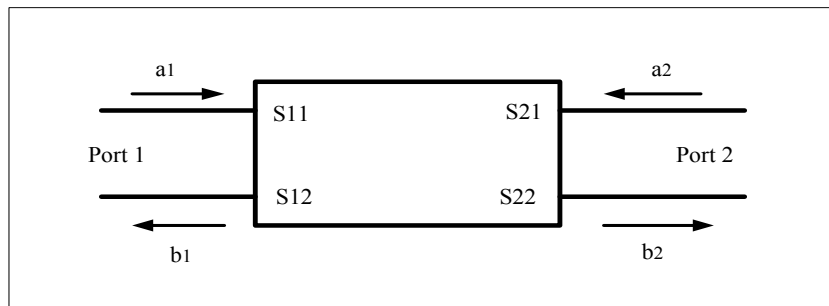
Figure 2.6: Scattering matrix of a two-port network [4]

Because the power line network is an interconnection of several two-port networks, it is then convenient to define the corresponding 2×2 transmission or the $ABCD$ matrix [2].

For the two-port network shown in Figure 2.7, the $ABCD$ matrix can be defined by [2, 48]:

$$\begin{bmatrix} V_1 \\ I_1 \end{bmatrix} = \begin{bmatrix} A & B \\ C & D \end{bmatrix} \begin{bmatrix} V_2 \\ I_2 \end{bmatrix} \tag{2.35}$$

where I_1, V_1, are the input current and voltage, while I_2, V_2 are the output current and voltage of the network respectively.
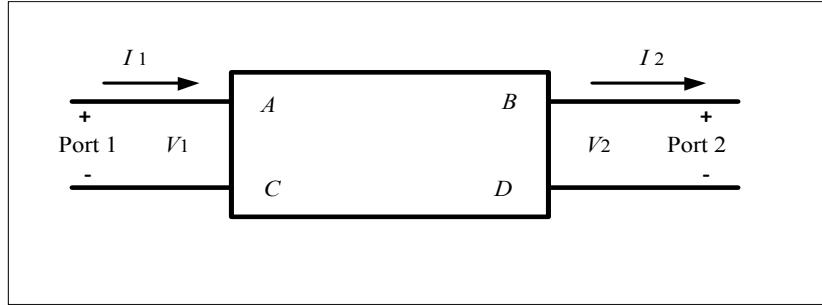
Figure 2.7: $ABCD$ matrix of a two-port network [1, 2]

We then convert from the S-matrix to the $ABCD$ matrix through the following equations [2]:

$$A = \frac{(1 + S_{11})(1 - S_{22}) + S_{12}S_{21}}{2S_{21}} \tag{2.36}$$

$$B = Z_o \frac{(1 + S_{11})(1 + S_{22}) + S_{12}S_{21}}{2S_{21}} \tag{2.37}$$

$$C = \frac{1}{Z_o} \frac{(1 - S_{11})(1 - S_{22}) - S_{12}S_{21}}{2S_{21}} \tag{2.38}$$

$$D = \frac{(1 - S_{11})(1 + S_{22}) + S_{12}S_{21}}{2S_{21}} \tag{2.39}$$

where Z_o is the cable characteristic impedance.

2.3 Multipath Propagation in Power Line Channel

For PLC, the transmission medium is the high-voltage low frequency power line network between the transmitter and the receiver [49]. Due to the presence of several impedance mismatched points along the power line channel and the 'ON' and 'OFF' connection of terminal loads into and out of the power line network, the transmitted signal undergoes geometric spreading and scattering of the electromagnetic energy. This results in scattered signal energies arriving at the receiver via different paths with different time delays, hence multipath propagation. To determine and understand the extent of multipath propagation, we determine the associated multipath characteristics of the channel.

2.3.1 Multipath Characteristics of the PLC Channel

In order to analyse, understand and characterize the multipath effect in the power line channel, we employ analytical techniques from wireless channels to determine the multipath characteristics of the power line environment [50]. The well-known multipath problems of the power line channel include attenuation, time delay and several multipath numbers [36, 51]. The time delay problem has been of very much interest to several PLC researchers. This time delay problem is parametrized by: the Root Mean Square (RMS) delay spread, mean excess delay, maximum excess delay spread and the coherence bandwidth of received signal. All these parameters are extracted from the power delay profile of the received signal.

Thus, in a consolidated effort to describe the multipath phenomenon in PLC, several researchers [50], [51], [52], [53] among others have used complete analytical and simulation approach to determine the multipath delay parameters and statistics, while [54], [55], [56], [57], [58], [59] have resorted to taking measurements and extracting the parameters from the measurement data.

2.4 PLC Channel Models

Channel models play one of the most important roles in the design of communication systems. Typical models undergo several iterations driven by simulation and measurement based evaluations and analysis [60]. Thus in PLC system, the top-down model and bottom-up model approaches have been presented to describe the channel models of the power line medium [16, 60, 61]. These different approaches are employed either in the frequency or time domains. In the bottom-up approach, the power line channel is first described by a mathematical model, then parameters of the model are computed and simulations done. Measurements are then carried out to validate the model. In addition, this model is based on transmission line theory model [46], in which the equivalent circuits of the differential mode [7] and the two-wire (live and neutral conductors) propagation along the power line are derived. The derived model is presented in terms of cascaded two-port networks or cascaded resonant circuits. This approach requires a detailed knowledge of the network topology, properties of the cables and load impedances which in reality are difficult to find or are never available. Because of this, the top-down model approach is always employed. In this approach, measurements of the power line channel is carried out first. From the measurement data, a model is then developed and parameters determined. In fact, this approach requires no prior knowledge about the topology, terminal load conditions and other details about the network. The most used model in top-down approach is a multipath model in which transmitted signal suffers multiple reflections, multipath fading and scattering as it propagates through the line. This multipath nature of the power line network arises from the presence of the multiple branches and several points of impedance mismatches. Analysis of these characteristics is done in frequency and time domains. In the frequency domain, the frequency selective fading characteristics of the power line

channel are examined, while the multipath propagation delay characteristics are analysed in the time domain.

In this dissertation, only the major models based on the two approaches are briefly discussed, while one acknowledges the various models that have been discussed and presented in the literature.

2.4.1 Philips Echo Model

This model was developed by Philips [5] in his pioneering work in PLC channel modelling. In this model, the power line channel is considered as a multipath channel due to the multiple reflections occurring at points of impedance discontinuities that cause echoes of the transmitted signal. Each transmitted signal reaches the receiver not only on the direct path, but also on other delayed and attenuated paths. Figure 2.8 shows the derived model.
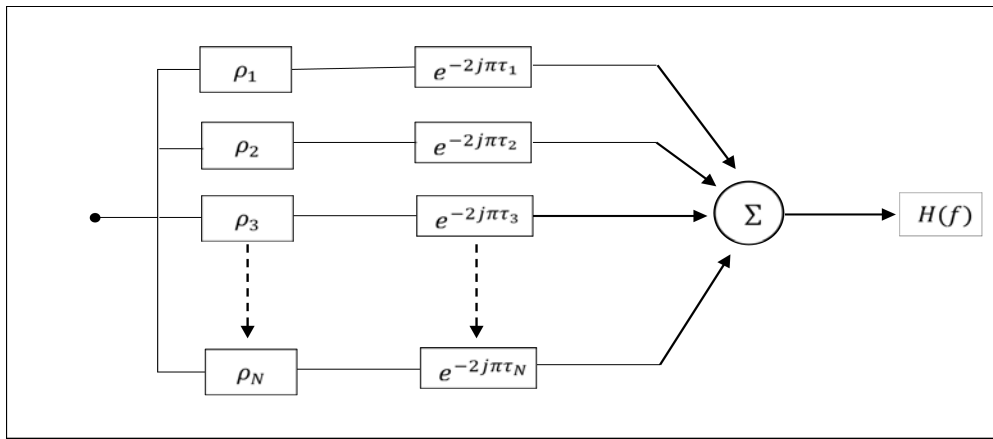
Figure 2.8: Conceptual sketch of Philips Echo Model [5]

In this model, the receiver receives signals through N paths, delayed by time τ_v , phase shifted by phase θ_v and attenuated by the complex factor ρ_v. The complex attenuation factor of each path is given by [5]:

$$\rho = |\rho_v|.e^{j\theta v} : where, \theta_v = arctan\left(\frac{Im(\rho_v)}{R_e(\rho_v)}\right) \tag{2.40}$$

The impulse response $h(t)$ is written as the sum of the N Dirac pulses multiplied by ρ_v, delayed by τ_v and given by [5]:

$$h(t) = \sum_{v=1}^{N} |\rho_v|.e^{j\theta v}.\delta(t - \tau_v) \tag{2.41}$$

The transfer function $H(f)$ is derived by performing a Fourier transformation on the

measured impulse response as [5, 7, 10]:

$$H(f) = \sum_{v=1}^{N} |\rho_v| . e^{-j2\pi f \tau_v} \qquad (2.42)$$

From the model, each path is described by an impulse response $h(t)$ causing a delay τ_v, an attenuation $|\rho_v|$ and a phase shift θ_v.

2.4.2 Philips Series Resonant Circuit (SRC) Model

This model was proposed by Philips [5] based on the impedance measurements of various electrical loads [27]. In this model, the loads are described by a few series resonant circuits that consist of a resistance R, capacitance C and inductance L. Hence, the power line channel is described as a cascade of decoupled series resonant circuits (SRC). This model is shown in Figure 2.9 with one SRC circuit connected to a line of impedance Z_o.
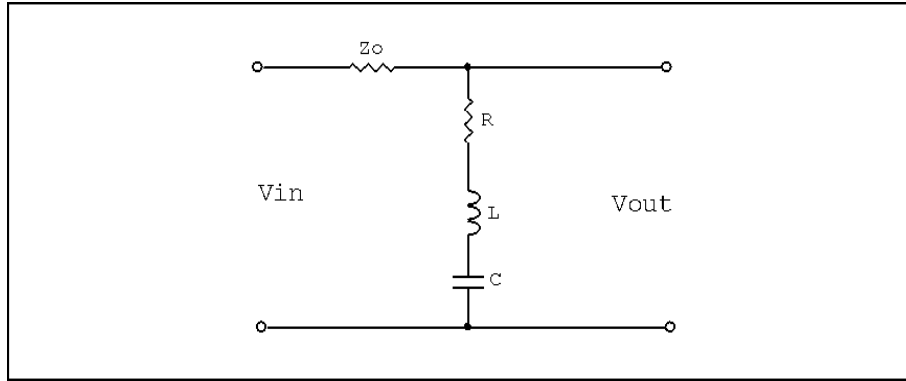
Figure 2.9: Philips SRC circuit [5]

From Figure 2.9, the frequency dependent impedance of the SRC circuit Z_s is given as [5]:

$$Z_s(f) = R + j2\pi f L + \frac{1}{j2\pi f C} \qquad (2.43)$$

At resonance, the frequency f_{res} will be [5, 27]:

$$f_{res} = \frac{1}{2\pi\sqrt{LC}} \qquad (2.44)$$

The transfer function $H_i(f)$ for each of the resonant circuits is given by [5]:

$$H_i(f) = \frac{Z_s(f)}{Z_s(f) + Z_o} \qquad (2.45)$$

The resulting transfer function is as shown in Figure 2.10. In this model, the notch in amplitude characteristics is seen at the resonant frequency.

20
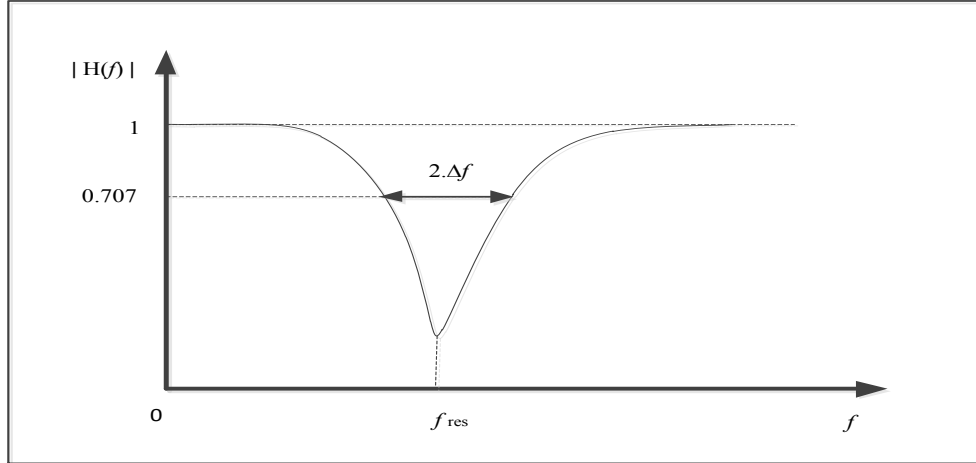
Figure 2.10: Amplitude characteristics of the SRC model [5]

The depth of the notch is dependent on the resistance R and impedance Z_o, while the width of the notch is determined by the quality factor Q of the notch which is equal to [5, 27]:

$$Q = \frac{1}{R} \cdot \sqrt{\frac{L}{C}} \qquad (2.46)$$

The transfer function of the power line channel is modelled as a cascade of N decoupled SRC circuits. Thus, the resulting overall transfer function $H(f)$ is given by [5]:

$$H(f) = \prod_{i=1}^{N} H_i(f) \qquad (2.47)$$

Each resonant circuit is described by three parameters: resistance R, inductance L and capacitance C. In this model, an evolutionary strategy is used to compute the optimised values of these parameters.

2.4.3   Zimmermann and Dostert Multipath Model

This model was adapted from [5] and developed by [6] to account for the attenuation of the transmitted signal as it propagated through the channel as given in (2.48). In this model, the power line channel is considered a 'black box' in the frequency range of 500 KHz to 20 MHz and described using a few parameters. This model is based on the physical signal propagation effects of the power line channel that include: multiple branches and impedance mismatches. In addition, the signal suffers reflections, frequency selective fading, multipath propagation and attenuation that increases with cable lengths and frequency. The multipath propagation phenomena is depicted in Figure 2.11.
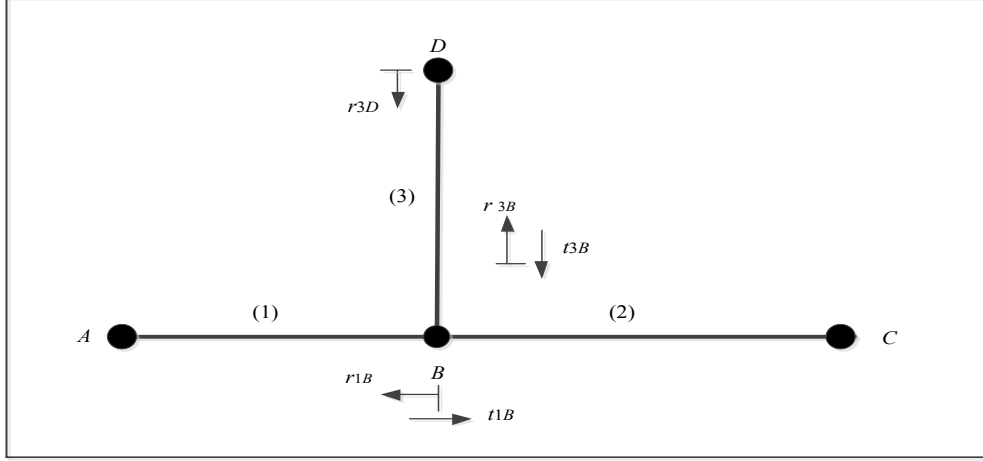
Figure 2.11: Multipath signal propagation: cable with one tap [6]

The link consists of the segments (1), (2), and (3) with lengths l_1, l_2, and l_3 with the characteristic impedances Z_{L1}, Z_{L2}, and Z_{L3}. The reflection factors are denoted by r_{1B}, r_{3D}, and r_{3B}, while the transmission factors are denoted, by t_{1B} and t_{3B}. Nodes A and C are assumed to be matched, meaning $Z_A = Z_{L1}$ and $Z_C = Z_{L2}$. This leaves the remaining nodes B and D as the reflection points. From (2.48), each path has a characteristic weighting factor g_i which is the product of the reflection and transmission factors with a path length d_i. The attenuation factor is derived from the parameters a_0, a_1, and k, which are obtained from measurement data and thus a top-down approach. In Figure 2.11, a signal is injected at the node A and propagation occurs towards point B. Upon reaching point B, some signal will be reflected while others will be transmitted to the connected load at point C. This process is continuous [6, 7].

This model, as shown in Equation (2.48) was extended to the bottom-up model as well. In this analytical approach, the parameters are derived from actual networks by taking into consideration the connected loads. The resulting model is described by (2.49) [6]:

$$H(f) = \sum_{i=1}^{N} g_i . e^{-(a_0 + a_1 f^k).d_i} . e^{-j2\pi f \frac{d_i}{v_p}} \tag{2.48}$$

$$H(f) = \sum_{i=1}^{N} g_i(f).A(f,d).e^{-j2\pi f \tau_{d_i}} \tag{2.49}$$

With,

$$A(f,d) = e^{-(a_0 + a_1 f^k).d_i} \tag{2.50}$$

$$\tau_i = \frac{d_i \sqrt{\varepsilon_r}}{c_o} = \frac{d_i}{v_p} \tag{2.51}$$

Where: N is the number of propagation paths, g_i is the weighting factor, a_0, a_1, and exponent k are the attenuation parameters, d_i is the path length, τ_i is the path delay, ε_r is

the dielectric constant of the cable insulation, c_0 is the speed of light, v_p is the propagation speed and $A(f, d)$ is the attenuation factor.

2.4.4 Anatory *et al.* Model

In this model, the power line network is considered as a transmission line with multiple distributed branches at a single node B, as shown in Figure 2.12 [7,30,61]. Mathematically, this model's transfer function $H_m(f)$ is described as [7,30,61]:
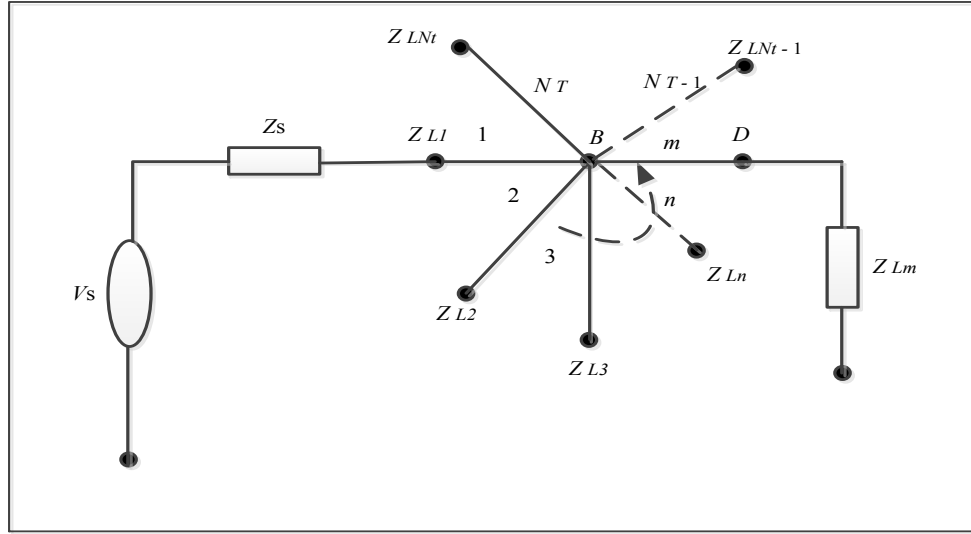
Figure 2.12: Power line network with multiple branches at a single node [7]

$$H_m(f) = \sum_{M=1}^{L} \sum_{n=1}^{N_t} T_{Lm} \alpha_{mn} H_{mn}(f), n \neq m \tag{2.52}$$

Where: n is the number of branches, m is the referenced terminated load, M is the number of reflections, $H_{mn}(f)$ is the transfer function between line n and referenced load m, T_{Lm} is the transmission factor at the referenced load m, N_t is the total number of branches connected at node B, L is the total number of reflections and α_{mn} is the contribution factor.

With the signal contribution factor α_{mn} at node B between line n and the referenced load m given by [7,30,61]:

$$\alpha_{mn} = P_{Ln}^{M-1} \rho_{nm}^{M-1} e^{-\gamma_n (2(M-1)l_n)} \tag{2.53}$$

Where: ρ_{mn} is the reflection factor at node B, γ_n is the propagation constant of line n that has a line length l_n and P_{Ln} is all terminal reflection factors.

The analysis is done with consideration of the effects of the power line network

branches, number of reflections resulting from these branching points, path distances and connected loads. All terminal reflection factors P_{Ln} in general are given by (2.54), except at source where $P_{L1} = \rho_s$ is the source reflection factor [7, 30, 61]. In addition, Z_s is the impedance of the source, with Z_n being the characteristic impedance of any terminal with source. V_s and Z_L are the source voltage and load impedance respectively. The output referenced voltage $V_m(f)$ across any load in the frequency domain is given by (2.55) [7, 30, 61]:

$$P_{Ln} = \begin{cases} \rho_s & n = 1(\text{source}) \\ \rho_{Ln} & \text{otherwise} \end{cases} \tag{2.54}$$

$$V_m(f) = H_m(f).\left(\frac{Z_{Ln}}{Z_{Ln} + Z_s}\right)V_s \tag{2.55}$$

For a more generalized case, a network with several distributed branches as shown in Figure 2.13 is considered. The transfer function is given by (2.56) and the parameters used bear similar meaning to (2.52) [7, 30, 61]:
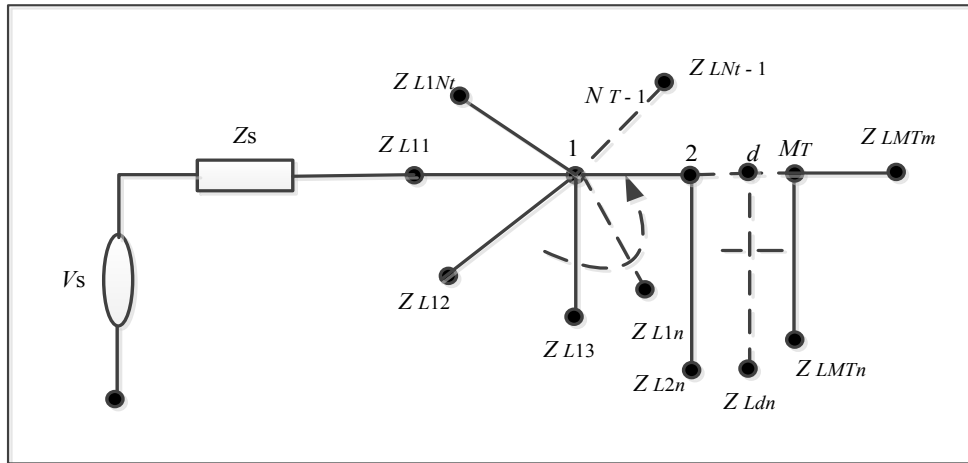
Figure 2.13: Power line network with distributed branches [7]

$$H_{mM_T}(f) = \prod_{d=1}^{M_T} \sum_{M=1}^{L} \sum_{n=1}^{N_T} T_{Lmd}\alpha_{mnd}H_{mnd}(f), n \neq m \tag{2.56}$$

With:

$$\alpha_{mnd} = P_{Lnd}^{M-1}\rho_{nmd}^{M-1}e^{-\gamma_{nd}(2(M-1)l_{nd})} \tag{2.57}$$

And:

$$P_{Lnd} = \begin{cases} \rho_s & d = n = 1(\text{source}) \\ \rho_{Lnd} & \text{otherwise} \end{cases} \tag{2.58}$$

$$V_{mM_T}(f) = H_{mM_T}(f).\left(\frac{Z_{Ldn}}{Z_{Ldn} + Z_s}\right)V_s \tag{2.59}$$

24

Where: M_T is the total number of distributed nodes, d is any referenced node $(1 \cdots, M_T)$ and $H_{mnd}(f)$ is the transfer function from line n to a referenced load m at node d.

2.4.5 Series Resonant Circuit (SRC) Model [Proposed by Zwane and Afullo]

In this model, the PLC channel is described as a cascade of series resonant circuits (SRC), with each SRC connected to a line with a characteristic impedance Z_o in the frequency range of 1-30 MHz as shown in Figure 2.9. The bottom-up approach is used in this model to design and implement the PLC network. Because the PLC channel is time and frequency variant, it is difficult to track the load impedances at multiple branch terminals as done in [5]. It is therefore, for this reason that this model analyses the input impedance characteristics of the PLC channel around a resonant wavelength λ_r [3, 10]. In addition, the impedance of the frequency dependent SRC $Z_s(f)$, resonant frequency points f_res and quality factor Q are given as (2.43), (2.44) and (2.46) respectively. The individual SRC circuits transfer function $hri(f)$ are given by (2.60) with (2.61) giving the transfer function for a multiple of n resonant points along a single branch length [3,10]. The overall network transfer function composed of N number of branches in a given network is thus given by (2.62) [3,10]. Also, the attenuation factor is considered in the transfer function, unlike in the Philips model [5] in which this factor is assumed.

$$hri(f) = \frac{Z_s(f)}{Z_s(f) + Z_o} \tag{2.60}$$

$$Hri(f) = \prod_{i=1}^{n} hri(f) \tag{2.61}$$

$$H(f) = A \prod_{i=1}^{N} Hri(f) \tag{2.62}$$

Where A is the attenuation factor dependent on the frequency f of signal transmission and path length l of the branch [3, 10].

To obtain the values of the three parameters: resistance R, inductance L and capacitance C, transmission line resonant circuit theory is employed. Table 2.1 show the parameters of the model.

Table 2.1: Series resonance RLC parameters [3, 10]

Parameters	Quarter wavelength ($\lambda_r/4$)	Parameters	Half wavelength ($\lambda_r/2$)
R	$\frac{1}{4}Z_o\alpha\lambda_r$	R	$\frac{1}{2}Z_o\alpha\lambda_r$
L	$\frac{\pi Z_o}{4\omega_o}$	L	$\frac{\pi Z_o}{2\omega_o}$
C	$\frac{4}{\pi\omega_o Z_o}$	C	$\frac{2}{\pi\omega_o Z_o}$
Q	$\frac{\beta_r}{2\alpha}$	Q	$\frac{\beta_r}{2\alpha}$

Where: Z_o is the cable characteristic impedance, ω_o is the angular frequency of the resonant point, α is the attenuation constant of the line, λ_r is the wavelength at the point of resonance and β_r is the phase constant of the signal at resonance [3, 10].

2.4.6 Multipath Model [Proposed by Modisa and Afullo]

This model employs a top-down approach in which the PLC channel is considered a multipath propagation environment with frequency selective fading. The power line channel is characterised and modelled in the frequency band of 1 - 30 MHz based on channel transfer function measurement results from a typical power line network as presented in [8]. This model is based on Zimmermann and Dostert model presented in [6] and describes the frequency response of the network topology with precision. The model is described by [8]:

$$H(f) = \sum_{i=1}^{N_i} g_i \cdot (f)^{-j\frac{2\pi d_i}{v}f} \cdot A(f, d_i), 0 \le B_1 \le f \le B_2 \tag{2.63}$$

where N_i is the number of paths, $g_i(f)$ is the complex and frequency dependent transmission/reflection factor for path i. The path length is given by d_i, while $v = c/\sqrt{\varepsilon_r}$, with c being the speed of light and ε_r defining the cable's dielectric constant. The cable losses result in attenuation $A(f, d_i)$ due to increase in cable length and frequency. This attenuation is simplified as given in Equation (2.50) resulting in a reduced PLC transfer function given by [8]:

$$H(f) = \sum_{i=1}^{N_i} g_i \cdot (f)^{-j\frac{2\pi d_i}{v}f} \cdot e^{-(a_o + a_1 f^k)d_i}, 0 \le B_1 \le f \le B_2 \tag{2.64}$$

with the parameters a_o, a_1, K, and N_i defining the model for adoption to a specific PLC network. Table 2.2 gives a summary of these parameters and their values for three different channels.

Table 2.2: Model parameters for three channels [8]

Channel #	Parameters			
	$a_o(m^{-1})$	$a_1(s/m)$	N_i	K
1	$5e^{-3}$	$2e^{-11}$	50	0.8
2	$2.5e^{-3}$	$5.5e^{-9}$	40	0.8
3	$4e^{-3}$	$2e^{-11}$	15	0.8

2.4.7 Proposed Parallel Resonant Circuit (PRC) Model

With the models presented in [5] and [10] as the basic foundational models, a model employing parallel resonant circuits (PRC) is then proposed in this study. In this model, the bottom-up approach is used. Transmission line resonant circuit theory is employed to determine the RLC parameters, simulations on network designs done, networks built and measurements done to validate the model. The designed and built networks for the

26

validation of the proposed model and measurement procedures are presented in chapter 3, while the analysis, simulation and measurement results are presented in chapter 4.

2.4.8 Proposed Multipath Propagation Characteristics Analysis

Due to lack of knowledge on the complex structure and topology of the unknown power line networks, we resort to the top-down approach in our analysis and investigations on the characteristics of the power line channel in the time domain. Measurements of the power line channel transfer functions are taken in selected locations within the University of KwaZulu-Natal, and an Inverse Discrete Fourier Transformation (IDFT) done to obtain the corresponding impulse responses. From the impulse response results, the time variant and multipath propagation parameters are extracted. The concept, analysis and results are presented in detail in chapter 5.

2.5 Chapter Summary

In this Chapter, we have studied the fundamentals of wave propagation in power transmission lines based on the well-established two-wire transmission line theory and the two-port circuit model by the use of scattering and $ABCD$ matrices. In addition, we have also studied the power line channel based on the knowledge and concepts of multipath propagation. The key fundamental contributions and literature in the field of PLC channel modelling and characterization have also been reviewed. In our study, two distinct approaches in the study and characterization of the power line channel as communication medium are presented. That is; the bottom-up and top-down approaches. The bottom-up approach involves establishing parameters, simulation of models and validation through measurements. On the other hand, the top-down approach involves performing measurements and extracting models and parameters from measurement data. With the knowledge of these two approaches in mind, a model based on the bottom-up approach is proposed and its concept explained in detail in the preceding chapter 4. On the other hand, through the top-down approach, an existing multipath model concept is proposed for the analysis of the PLC channel multipath propagation characteristics and will be fully discussed in chapter 5.

Chapter 3

MEASUREMENT PLANS AND PROCEDURES

3.1   Introduction

In this chapter, we present the 9 KHz - 13.6 GHz Rohde & Schwarz ZVL13 Vector Network Analyzer (VNA) measuring instrument, the couplers used, the measurement set-ups and procedures followed in the course of this research. We also present the operations of the VNA by means of typical network configurations and measurements. In this research, measurement process is of utmost importance. It is through measurements that we carry out validation of the designed and simulated model developed in preceding chapter 4 besides analysis of the multipath propagation characteristics of the power line channel from measurement data as presented in chapter 5. This therefore calls for very efficient and consistent measurement procedures and instrumentation process using the analyzer as the main instrument in addition to the peripherals that include: PLC couplers, connectors, and power line networks.

3.2   Rohde & Schwarz ZVL13 Vector Network Analyzer

Measurements were done using the Rohde & Schwartz ZVL13 Vector Network Analyzer (VNA) shown in Figure 3.1 to obtain the channel complex frequency responses in the frequency band of 1-30 MHz.

Figure 3.1: Rohde & Schwarz ZVL13 VNA

This analyzer provides numerous functions to perform specific measurements, customize and optimize the evaluation of results. It is suitable for reflection measurements as it transmits a stimulus signal to the input port of the device under test (DUT) and measures the reflected wave. The instrument uses a hierarchy of structures to ensure that the instrument resources are easily accessible and that user-defined configurations are conveniently implemented, stored and reused. The VNA is capable of performing the following measurements [4]:

- S-parameters: These are the basic measured quantities by the VNA. They describe how a transmitted or reflected signal in either forward or reverse directions undergo modification by the DUT. The S-parameter S_{21} was selected as the measurement parameter all through our measurements.

- Impedance parameters: Impedance is a complex ration of voltage and current. This VNA provides matched-circuit impedances converted from the reflection S-parameters.

- Converted impedances: The converted matched-circuit impedances, describe the impedances of a DUT that is terminated at its outputs with a reference impedance. The VNA converts the measured S-parameters to determine the matched-circuit impedances.

- Admittance parameters: Admittance is the complex ratio between a current and a voltage. This VNA provides matched-circuit admittances converted from the S-parameters.

- Converted admittance parameters: The matched-circuit converted admittances, describe the admittances of a DUT that is terminated at its outputs with the reference impedance values. This VNA converts the measured S-parameters to determine the matched-circuit admittances.

This VNA provides several tools for setting the sweep range. The sweep range refer to continuous range of the sweep variables that include; frequency, power and time containing the sweep points where the VNA takes measurements. In a segmented frequency sweep, the sweep range can be composed of several parameter ranges or single points [4].

To store and record the measurement data on the external storage device, the analyzer processed the measured data in a sequence of stages to obtain the displayed trace. The trace settings specified the mathematical operations used to obtain traces from the measured data. Each trace was assigned to a channel that contained hardware-related settings to specify how the network analyzer collected data [4]. The stored measurement data was accessed through the analyzer's Universal serial bus (USB) connectors, which are used to connect external storage devices for further external processing and analysis.

3.3   Calibration Procedure for the VNA

Calibration refers to the process of system error correction to the measuring instrument. The analyzer provided advanced and systematic calibration process for all the types of measurements. Calibrations were done using calibration kit ZV-Z21 that contained the appropriate male short standard with known physical properties. Due to the analyzer's calibration wizard through the use of the CAL function, calibration was a straightforward, menu-guided process. A calibration process employing four known standards TOSM (Through, Open, Short, Match) error correction model, available for 2, 3 and 4-port measurements was used.

TOSM calibration standard has the highest accuracy and is the most applicable for reflection and transmission measurements on DUT with two ports.

3.4   Coupler and Coupling for Measurements

Similar to other communication systems, coupling and impedance matching is a very important aspect and area in PLC communications. This is so because properly matched PLC modem or measuring equipment to the ever varying power line impedance ensures integrity of our information signal from the channel noise, attenuation and other impairments.

The area of coupling and impedance matching in PLC communication requires a deeper understanding of design and manipulation of filters to achieve the level of impedance that will ensure integrity of transmitted information. It is for this reason that several researchers [62], [63], [64], [65] and [66], are also involved in this aspect of PLC research work. Hence, in this section we present the coupler and its application to measurements.

3.4.1 PLC Coupler

A differential mode coupler constructed and presented in [3], [8], [10], [46] were used in which, one terminal were connected to the live conductor while the other terminal were connected to the neutral conductor. The functions of the coupler are:

- Isolation of the measuring instrument from the mains high-voltage electrical power supply network thus ensuring safety of the equipment and personnel.

- Blocking the 50 Hz frequency signal and other noise signals from the mains electrical power supply network.

- Provides points for injecting and extracting the low-voltage high frequency data signal into and from the electrical power supply network.

- To achieve impedance matching between the fixed impedance at the terminal ports of the measuring instrument and the ever varying line impedance of the mains electrical power supply network.

From Figure 3.2, the above functions are provided for by: a broadband isolation transformer of a 1:1 winding ratio in combination with filter capacitors forming high pass filters on both primary and secondary sides of the transformer and two back-to-back connected zener diodes that limit the output voltage levels. A transient voltage surge suppressor (TVSS) is also connected on the primary of the transformer for surge protection.
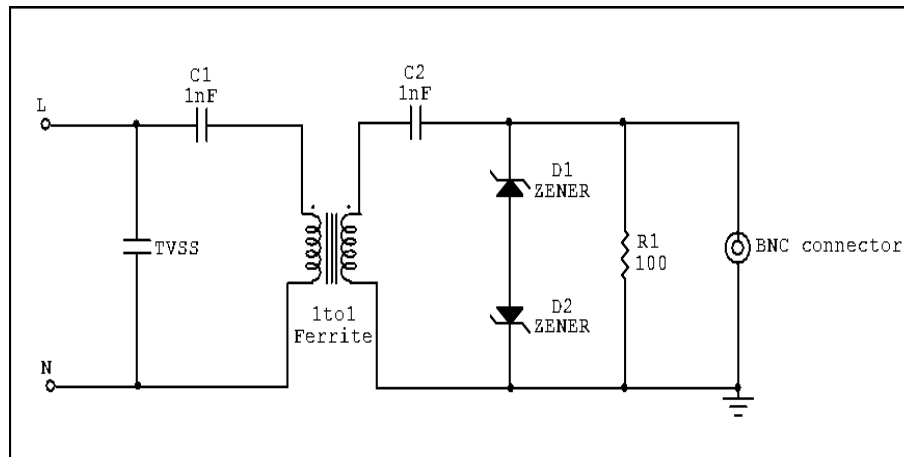
Figure 3.2: PLC Coupler schematic diagram [3,8]

Figure 3.3 shows the complete assembled bidirectional couplers used in this research for measurements. These couplers exhibited transfer characteristics with flat responses in the frequency band of 1-30 MHz as shown in Figure 3.4.

31

Figure 3.3: Complete assembled PLC Couplers
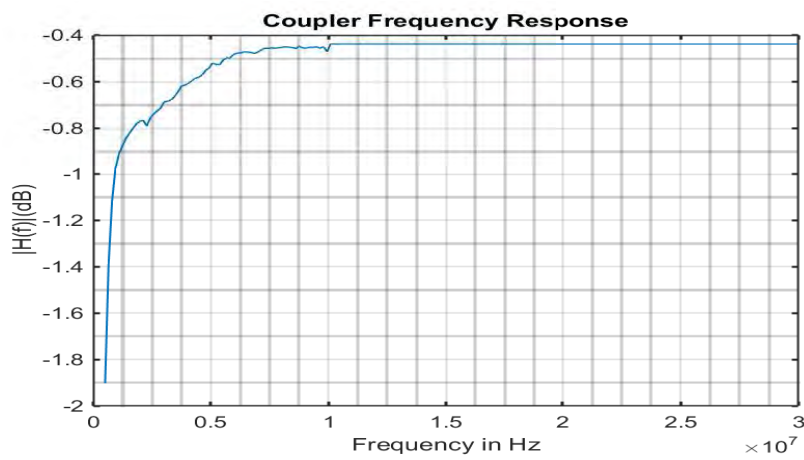
Figure 3.4: Coupler frequency response

3.4.2 Coupling for Measurements

To connect the analyzer to the couplers, the N-connectors labelled PORT 1 and PORT 2/ RF INPUT shown in Figure 3.5 (a) were connected to the BNC terminated couplers using BNC to N-connector adaptors shown in Figure 3.5 (b). These ports served as output for the RF stimulus signal and as input for the measured RF signals from the network. The couplers were then plugged into the power line network through the socket outlets. The complete connection set-up were as shown in Figure 3.6. With these two ports, it was possible to perform full two-port measurements and obtain the respective S-parameters.
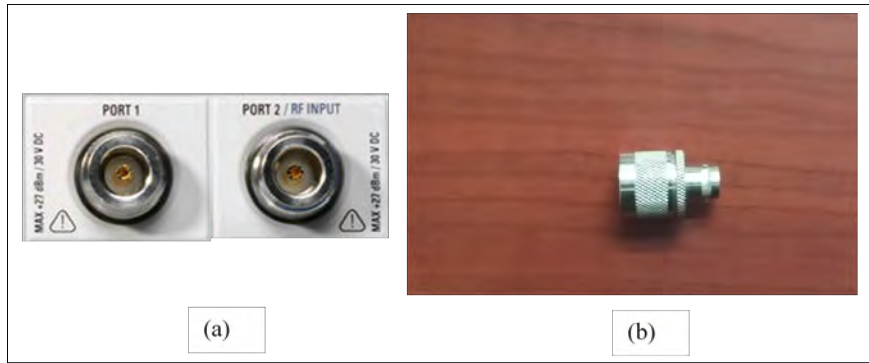
Figure 3.5: (a) VNA N-connector ports [31]. (b) BNC to N-connector
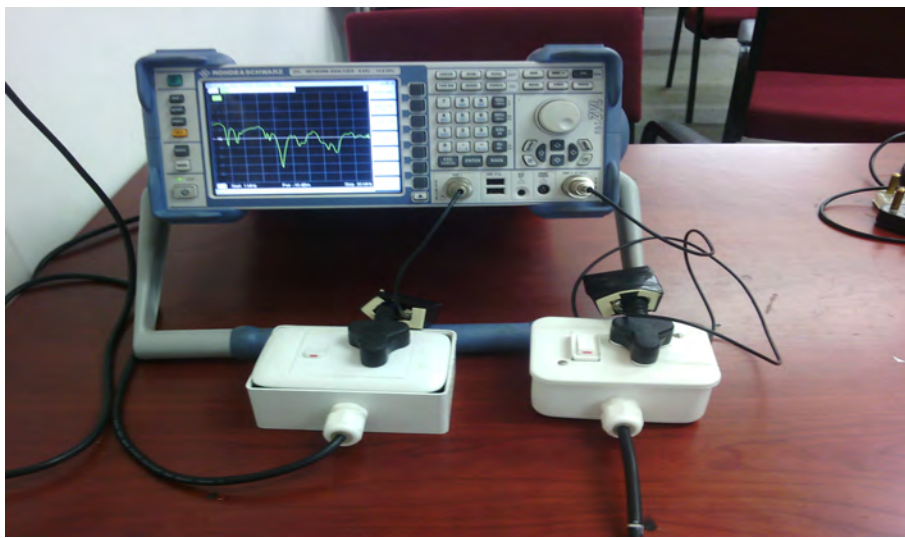
Figure 3.6: Couplers connected to the analyzer ports through BNC to N-connectors

3.5   Measurement Set-up for Network Measurements

After calibration of the VNA, a frequency sweep range of 1-30 MHz were set, and the S_{21} parameter selected as a measurement parameter. The networks where measurements were done were categorized into two: known network topologies and an unknown network topologies.

3.5.1   Known Network Topologies

The known network topologies are the networks whose characteristics and parameters that included, frequency resonant points, the RLC resonant circuit parameters and branch lengths were designed and known. In addition, the electrical power supply to these networks were through the on-line uninterruptable power supply (UPS) that provided a constant mains voltage. The measurement set-up shown in Figure 3.7 were used for validation of the designed and simulated channel model as presented in chapter 4. The

design and wiring schematics are also discussed in the same chapter.

Figure 3.7: Measurement set-up for Known Network topologies

3.5.2 Unknown Network Topologies

Unknown network topologies are the power line networks whose network parameters and configurations were not available and not known. They included selected offices, laboratories and workshop locations within the University of KwaZulu-Natal where measurements were done. The measurement set-up used in all the selected unknown networks is as shown in Figure 3.8.

Figure 3.8: Measurement set-up for all unknown Networks

The unknown network topologies that were investigated are as follows:

- Second Year Electrical, Electronic and Computer (EEC) Engineering Laboratory

In this location as shown in Figure 3.9, a workstation was composed of a function generator, a digital multimeter, an oscilloscope and a trainer. The network connection was such that three workstations were connected to a single circuit breaker at the Distribution Board (DB) forming a single network. Thus measurements were done for a single network and two combined networks which translated into six workstations.

Figure 3.9: Second Year EEC Engineering laboratory

- Second Year EEC Engineering Computer Laboratory

In this laboratory as shown in Figure 3.10, the network connection was such that six workstations were connected to a single circuit breaker at the DB board forming a single network. A workstation had a CPU and a monitor. Thus measurements were done for a single network and two combined different networks having twelve workstations.

Figure 3.10: Second Year EEC Computer laboratory

- Offices

  Based on the knowledge of power supply network connections from the other
  locations from the DB boards, a random check on the network connections in several
  offices was done and it was found that the offices had single networks. The problem
  was fully establishing as to whether the power supply circuits in a single office were
  connected to a single circuit breaker at the DB or were just a loop from another next
  office since the installation schematics were unavailable. The selected office shown
  in Figure 3.11 had the most used office equipment in the engineering north building
  that included: an electric paper shredder, computer station, photocopier machine,
  a scanning machine, a laptop and a fax machine. And thus only this selected office
  result is presented.

Figure 3.11: An office

- Electrical Engineering Workshop

  This workshop had the most complex network amongst all the locations. Most heavy
  machinery had their own isolators or connected to a specific circuit breaker from a
  sub distribution board. With such connections, the network was composed of several
  sub-networks terminating at different circuit breakers at the main DB and isolators.
  The workshop is shown in Figure 3.12.

Figure 3.12: Electrical Engineering Workshop

The measurement set-up shown in Figure 3.8 was exclusively used in chapter 5, in which we define and investigate the multipath propagation characteristics of the power line network channel.

3.6 Chapter Summary

In PLC research, measurements form an integral tool and part of the research procedures besides computer based simulations. It is from actual measurements that, we are able to validate simulated models and to fully observe and understand how the power line channel characteristics affect signal propagation. And thus, in this chapter we have presented all the tools, instruments and procedures that are to be used and followed in the course of this research for measurements and data collection. Lastly, the networks under investigation have also been presented.

Chapter 4

PLC CHANNEL MODELLING USING PARALLEL RESONANT CIRCUITS APPROACH

4.1 Introduction

The electrical power supply networks are viewed as alternative channels for broadband data transmission due to the increased demand for high capacity data communication networks. This is attributed to the fact that the electrical power supply network infra-structure is in existence and no more costs are incurred in the set up and installation. As a result, the electrical power line is transformed into a multifunctional medium for the delivery of electrical energy, voice and data communication services. Because of the considerable difference in topology, structure and physical properties from the normal and conventional wired transmission mediums like coaxial cable, fibre optic cables or twisted pair cables [61], the electrical power line network presents a very harsh and unfavourable environment for high frequency digital communication. In the recent research and development of the low-voltage electrical power line network for communication of high frequency data signals, various modelling techniques have been used to characterize this network with design parameters being informed by the properties of the channel transfer characteristics and capacity offered by the channel [6, 10, 61]. This then calls for accurate models that can best describe the characteristics and transmission behaviour over the power line channel with sufficient precision [10, 67]. Currently, there is no universal standard model for the PLC channel. Several techniques to model the transfer characteristics of the power line network as a channel have been presented in literature. The two common approaches used to model the power line network are the top-down and bottom-up approaches. The models presented in [5, 6, 8], among other researchers, employs the top-down approach by using measurement data to model and calculate the component parameters of the models. In [10], [56], [61], [67], [68] the bottom-up approach is used where the power line network is characterized, parameters calculated and models defined.

The objective of this chapter is to investigate and model the power line characteristics as a channel for data communication in the frequency band of 1-30 MHz using the bottom-up approach. Transmission line parallel resonant circuit (PRC) is used to obtain the model parameters and then the results are compared to the series resonant circuit (SRC) model presented in [3, 10]. In these two models, the cable is assumed to support

transverse electromagnetic mode (TEM) propagation only. In [5] an evolutionary approach is employed to obtain the optimized component parameters of the presented SRC model. In this research, we use the power line cable primary parameters that were obtained and presented in [3, 29]. These parameters include: power line cable characteristic impedance, Z_o, propagation constant, γ, attenuation constant, α, and propagation velocity, v_p.

4.2   Transmission Line Resonant Circuit

At high frequencies of signal transmission, the usual lumped LC resonant circuits are replaced by open or short circuited sections of transmission lines [2, 9, 47]. By analysing the input impedance characteristics around the resonant wavelengths of the circuits of Figure 4.1, we can confirm that these circuits behave and possess the characteristics of a parallel resonant circuit [2, 9, 47].
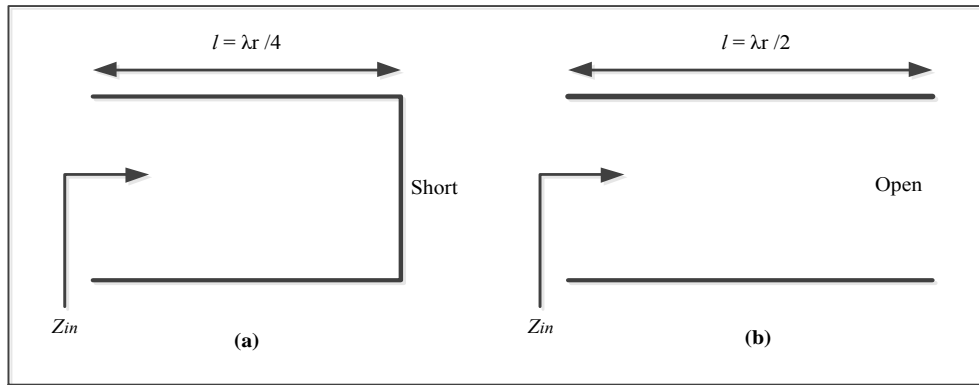
Figure 4.1: Types of transmission line parallel resonant circuits with length (a) a quarter wavelength. (b) a half wavelength [9]

In this section, the study and quantitative analysis of a resonant transmission line section is presented. We derive the parameters of the model with an assumption that the cable supports TEM mode signal propagation only [69].

4.2.1   Parallel Resonant Circuit (PRC) Model

A practical transmission line cable is as shown in Figure 4.1. This line will behave as a PRC when the length is in odd multiples of $\lambda_r/4$ or in even multiples of $\lambda_r/2$. The input impedance Z_{in} from Figure 4.1 that will be seen by the signal is given as (2.27). For $\alpha l \ll 1$, $tanh(\alpha l) \approx \alpha l$, and assuming a TEM mode only, $\beta l = \omega l/v_p$. Thus around the resonant frequency, ω_o, it can be simplified as [2, 9, 47]:

$$\beta l = \frac{\omega l}{v_p} = \frac{\omega_o l}{v_p} + \frac{\delta \omega l}{v_p} \tag{4.1}$$

39

$$= \beta_r l + \frac{\delta \omega l}{v_p} \tag{4.2}$$

with β_r being the phase constant at resonance.

If the transmission line is one-half-wavelength long at the resonant frequency, then [2, 9, 47]:

$$\beta_r l = \pi, and \frac{l}{v_p} = \frac{\pi}{\omega_o} \tag{4.3}$$

Therefore, $tan(\beta l)$ can be approximated as follows [2, 9, 47]:

$$tan(\beta l) = tan\left(\pi + \frac{\delta \omega l}{v_p}\right) = tan\left(\pi + \frac{\pi \delta \omega}{\omega_o}\right) \tag{4.4}$$

$$= tan\left(\frac{\pi \delta \omega}{\omega_o}\right) \approx \frac{\pi \delta \omega}{\omega_o} \tag{4.5}$$

and,

$$Z_{in} \approx Z_o \frac{\alpha l + j(\frac{\pi \delta \omega}{\omega_o})}{1 + j\alpha l(\frac{\pi \delta \omega}{\omega_o})} = Z_o\left(\alpha l + j\frac{\pi \delta \omega}{\omega_o}\right) \tag{4.6}$$

The assumption in (4.6) is that $\alpha l(\pi \delta \omega / \omega_o) \ll 1$.

For a $\lambda/4$ long transmission line at the resonant frequency, then [2, 9, 47]:

$$\beta_r l = \frac{\pi}{2}, and \frac{l}{v_p} = \frac{\pi}{2\omega_o} \tag{4.7}$$

Hence,

$$tan(\beta l) = tan\left(\frac{\pi}{2} + \frac{\delta \omega l}{v_p}\right) = tan\left(\frac{\pi}{2} + \frac{\pi \delta \omega}{2\omega_o}\right) \tag{4.8}$$

$$= -cot\left(\frac{\pi \delta \omega}{2\omega_o}\right) \approx -\frac{2\omega_o}{\pi \delta \omega} \tag{4.9}$$

and,

$$Z_{in} \approx Z_o \frac{-j\frac{2\omega_o}{\pi \delta \omega}}{1 - j\alpha l\frac{2\omega_o}{\pi \delta \omega}} = \frac{\frac{Z_o}{\alpha l}}{1 + j\frac{\pi}{\alpha l} \times \frac{\delta \omega}{2\omega_o}} \tag{4.10}$$

Now, using an equivalent PRC shown in Figure 4.2, the frequency dependent input admittance, $Y_{in}(f)$ seen by the input signal is given by [2, 9, 47]:
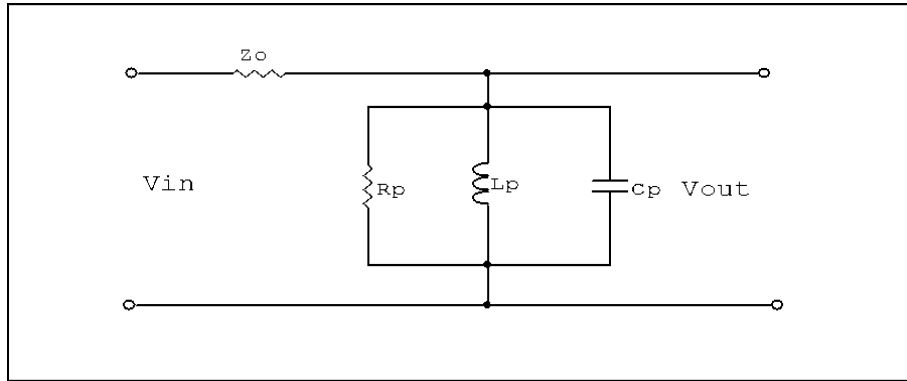
Figure 4.2: Equivalent Parallel Resonant Circuit [1]

$$Y_{in} = \frac{1}{Z_p} = \frac{1}{R_p} + j\omega C_p + \frac{1}{j\omega L_p} \tag{4.11}$$

$$= \frac{1}{R_p} + j\omega C_p\left(1 - \frac{\omega_o^2}{\omega^2}\right) \tag{4.12}$$

where Z_p, R_p, L_p and C_p are the parallel input impedance, resistance, inductance and capacitance respectively. For a lossy circuit, the input impedance will be equal to $1/R_p$ at resonance. Therefore, we can approximate the input impedance at resonance, $\omega_o \pm \delta\omega$ as follows [2,9,47]:

$$Y_{in} \approx \frac{1}{R_p} + j2\delta\omega C_p = \frac{1}{R_p} + j\frac{2\delta\omega Q}{\omega_o R_p} \tag{4.13}$$

Thus,

$$Z_p \approx \frac{1}{Y_{in}} = \frac{R_p}{1 + j\frac{2Q\delta\omega}{\omega_o}} \tag{4.14}$$

From these analysis, we observe a similarity between Equations (4.10) and (4.14). Therefore, this transmission line in Figure 4.1 is confirmed to be working as a PRC.

For a $\lambda/4$ short circuited transmission line, the equivalent RLC parameters are determined as follows [2,9,47]:

$$R_p \approx \frac{Z_o}{\alpha l} = \frac{4Z_o}{\alpha\lambda_r} \tag{4.15}$$

$$L_p \approx \frac{4Z_o}{\pi\omega_o} \tag{4.16}$$

$$C_p \approx \frac{\pi}{4\omega_o Z_o} \tag{4.17}$$

and,

$$Q = \frac{\pi}{4\alpha l} = \frac{\beta_r}{2\alpha} \tag{4.18}$$

For a $\lambda/2$ open circuited transmission line, the input impedance can be approximated by [2,9,47]:

$$Z_{in} \approx Z_o\frac{1 + j\alpha l(\frac{\pi\delta\omega}{\omega_o})}{\alpha l + j(\frac{\pi\delta\omega}{\omega_o})} = \frac{Z_o}{\alpha l + j\frac{\pi\delta\omega}{\omega_o}} \tag{4.19}$$

The equivalent RLC parameters are determined as follows:

$$R_p \approx \frac{Z_o}{\alpha l} = \frac{2Z_o}{\alpha\lambda_r} \tag{4.20}$$

$$L_p \approx \frac{2Z_o}{\pi\omega_o} \tag{4.21}$$

$$C_p \approx \frac{\pi}{2\omega_o Z_o} \tag{4.22}$$

and,

$$Q = \frac{\pi}{2\alpha l} = \frac{\beta_r}{2\alpha} \tag{4.23}$$

The computed parameters of the model are as in Table 4.1

Table 4.1: Parallel resonance RLC parameters [9]

Parameters	Quarter wavelength $(\lambda_r/4)$	Parameters	Half wavelength $(\lambda_r/2)$
R_p	$\frac{4Z_o}{\alpha\lambda_r}$	R_p	$\frac{2Z_o}{\alpha\lambda_r}$
L_p	$\frac{4Z_o}{\pi\omega_o}$	L_p	$\frac{2Z_o}{\pi\omega_o}$
C_p	$\frac{\pi}{4\omega_o Z_o}$	C_p	$\frac{\pi}{2\omega_o Z_o}$
Q	$\frac{\beta_r}{2\alpha}$	Q	$\frac{\beta_r}{2\alpha}$

Here, Z_o is the characteristic impedance of the power line cable, λ_r is the resonance wavelength, α is attenuation constant, R_p is the parallel resistance, L_p is the parallel inductance, C_p is the parallel capacitance, Q is the quality factor of resonance, $\beta_r = \pi/l$ is the phase constant at resonance and ω_o is the angular resonance frequency.

4.3 Channel Modelling in the Frequency Domain

4.3.1 Model Cable Lengths and Notch Positions

To establish the position and separation of the notches/resonant points along the transfer functions, we consider the electric length of the branches. A relationship expressed in terms of the wavelength, λ, propagation velocity, v_p and the signal frequency, f is then obtained as:

$$\lambda = \frac{v_p}{f} \tag{4.24}$$

For open circuit ended branches, the first notch will occur at a resonant frequency relative to the branch length, l given as [10, 27]:

$$f_o = \frac{v_p}{4l} \tag{4.25}$$

The following notches or resonant points along the open circuit branches are given by (4.26), while for the short circuit ended branches, the first notch occurs at zero and following frequencies occur as given by (4.27) [10, 27]:

$$f_{ok} = \frac{v_p}{4l}(2k+1) \tag{4.26}$$

$$f_{sk} = \frac{v_p}{4l}(2k) \tag{4.27}$$

with $k = 1, 2, 3, \cdots$, $v_p = 1.488 \times 10^8 ms$ and l is the branch length.

For a cascaded network configuration, the transfer function will be observed to follow a trend of addition in the transfer functions. Thus the transfer function can be calculated as [70, 71]:

$$H_{total}(dB) = H_{config1}(dB) + H_{config2} + \cdots + H_{configx}(dB) \tag{4.28}$$

42

where $x = 1, 2, 3, \cdots$

4.3.2 Parallel Resonant Circuit (PRC) Transfer Function

Having obtained the frequency dependent input impedance, $Z_p(f)$ in (4.14), the transfer function $hri(f)$ for each resonant circuit or point along the frequency span for a given length is given by [70, 71]:

$$hri(f) = \frac{V_{out}}{V_{in}} = \frac{Z_o}{Z_o + Z_p(f)} \tag{4.29}$$

Thus for n resonant circuits in a branch length, the transfer function $Hri(f)$ can be determined by [70, 71]:

$$Hri(f) = \prod_{i=1}^{n} hri(f) \tag{4.30}$$

Therefore, the overall network transfer function $H(f)$ is calculated by the product of all the branch transfer function can be expressed by:

$$H(f) = A \prod_{i=1}^{N} Hri(f) \tag{4.31}$$

Here, N is the number of branches in the network and A is the direct path attenuation factor from the transmitter to the receiver given by [6, 10]:

$$A(f, l) = e^{-(\alpha + j\beta)l} = e^{-(\alpha)l} \tag{4.32}$$

where α and β are the attenuation and phase constants of the power line from the propagation constant, f is the frequency of the signal and l is the direct path length from the transmitter to the receiver.

4.4 Simulation and Measurement Results

Simulation results for each of the network configurations using the PRC model are presented and compared to the SRC model presented in [3, 10]. The corresponding simulation and measurement results were obtained using network configurations in Table 4.2 for the SRC and PRC models respectively. Figures 4.3, 4.4 and 4.5 are the schematic wiring diagrams of the test bed networks used, while Figures 4.6, 4.7, 4.8, 4.9, and 4.10 are the results.

Table 4.2: Configurations for the Networks

Networks	Configurations	Transmit	Receive
Network 1	1	1	3
	2	1	2
Network 2	3	1	3
	4	1	4
Network 3	5	1	5
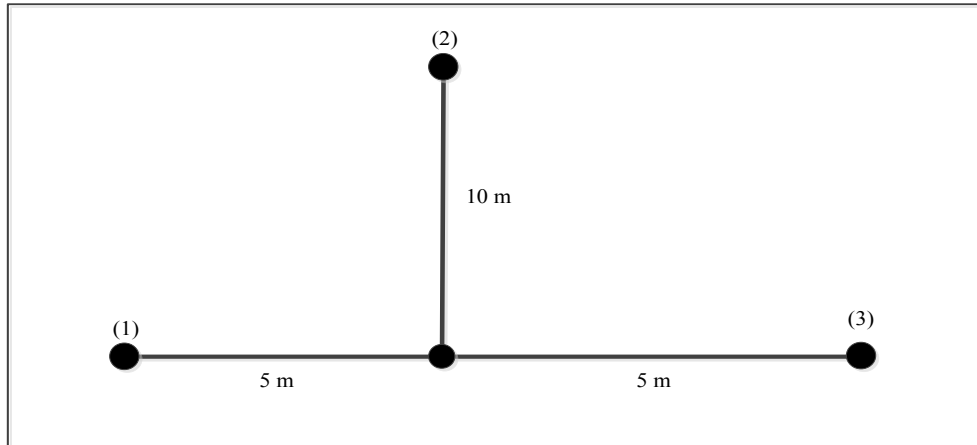
Figure 4.3: Network 1: Single T node branch network
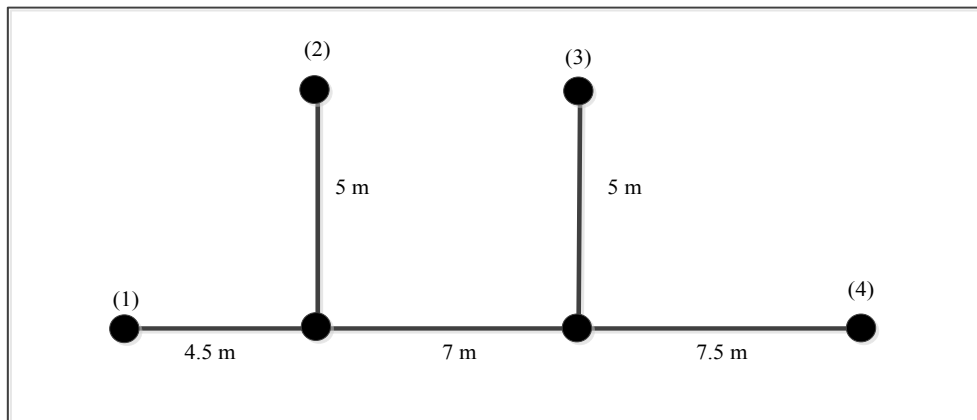
Figure 4.4: Network 2: Two T node branch network
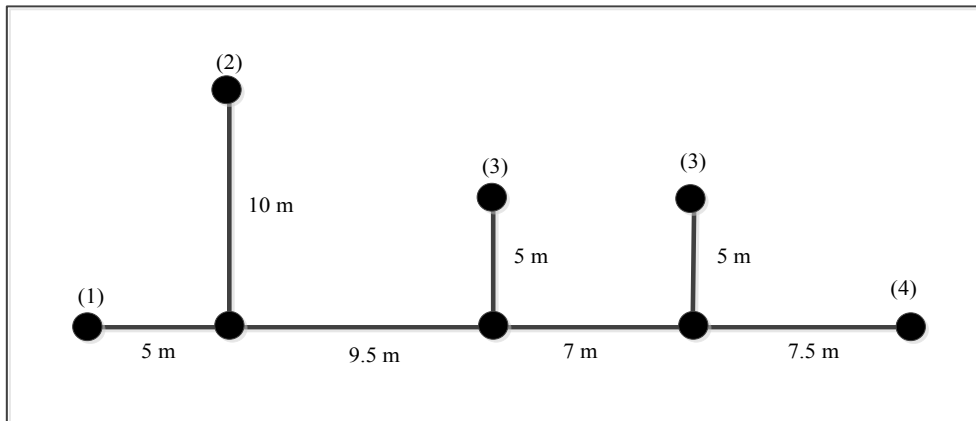
Figure 4.5: Network 3: Cascaded three T nodes branch network
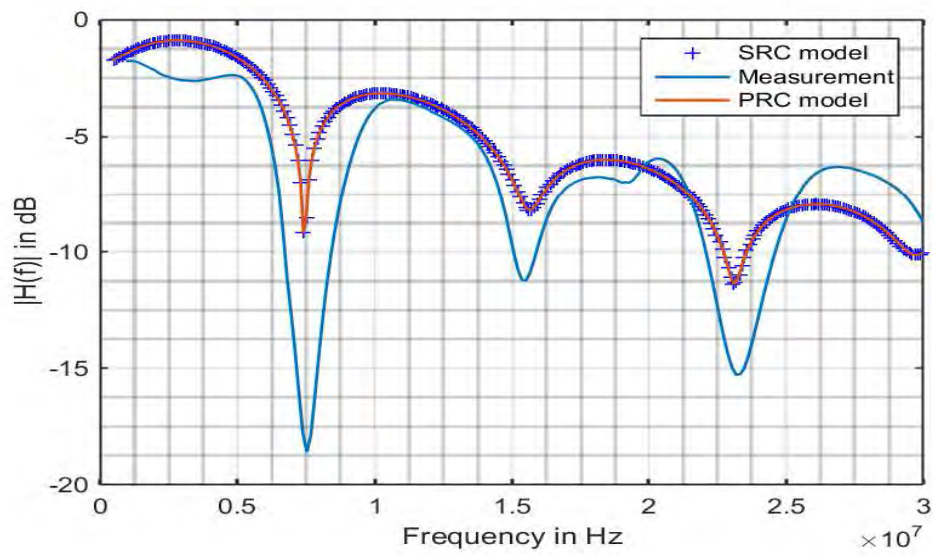
Figure 4.6: Configuration 1 results for network 1
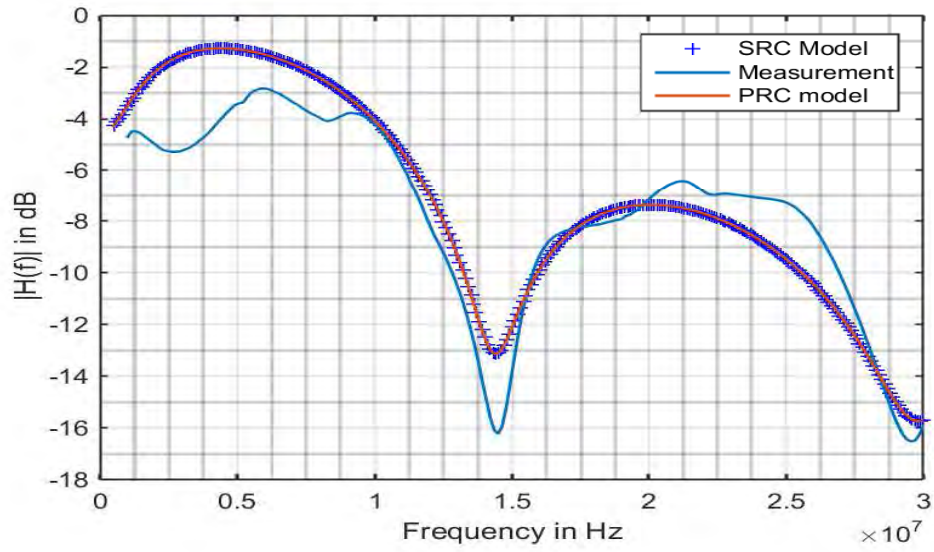
Figure 4.7: Configuration 2 results for network 1
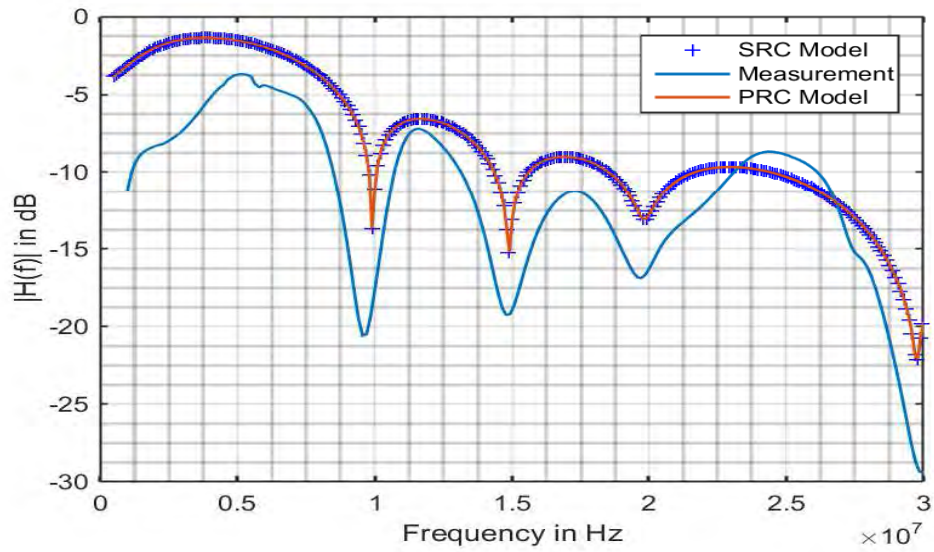
Figure 4.8: Configuration 3 results for network 2

46
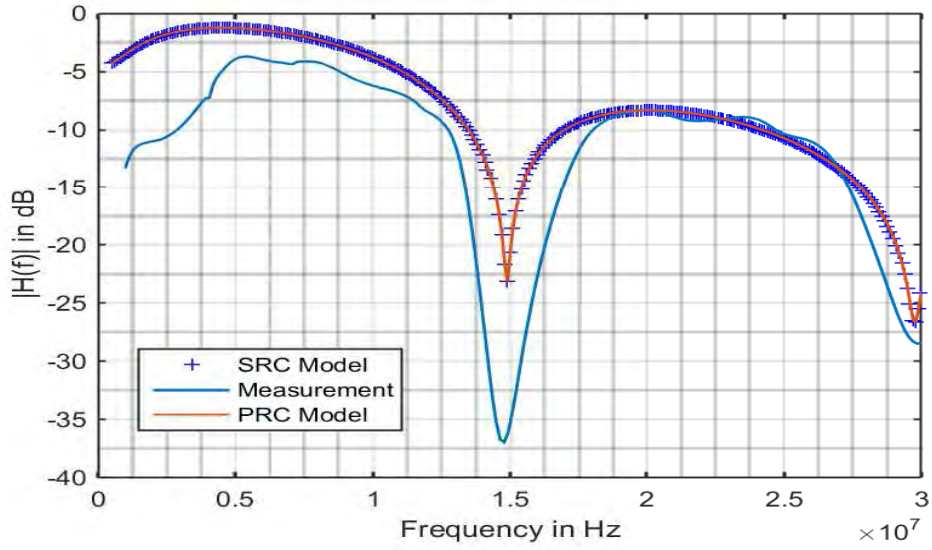
Figure 4.9: Configuration 4 results for network 2
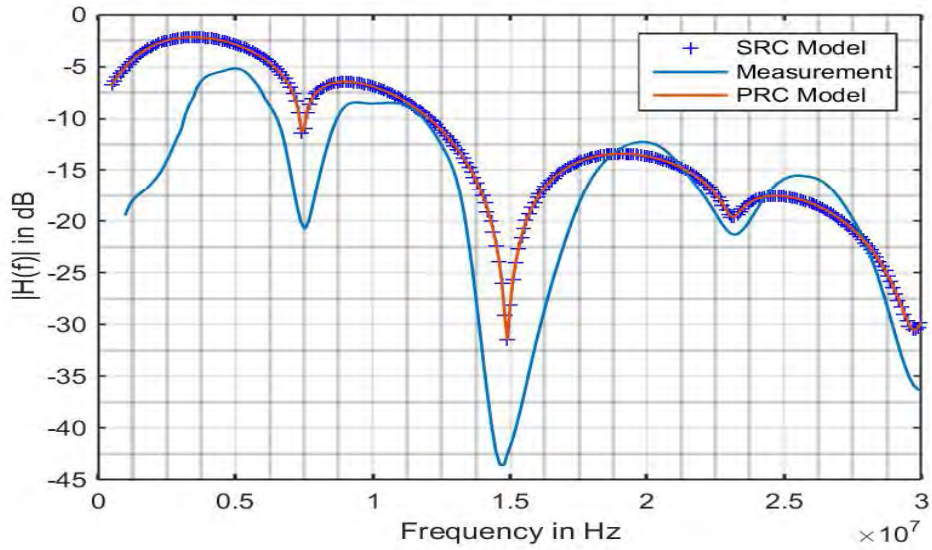
Figure 4.10: Configuration 5 results for network 3

Measurements were done on the constructed test bed networks at the PLC laboratory 131S as presented in chapter 3 using the VNA and data recorded for analysis.

4.5   Discussion of Results

From the transfer function results, it is seen that the number and depth of notches along the transfer function is dependent on the length of the branch for a single branch network. That is, the longer the branch, the more the number of notches with low depths as

compared to shorter branch lengths that have few number of notches but with more pronounced deep notches. It can also be observed that, having successive branches of the same length results in more pronounced and wider notches. This is not a desirable effect for data transmission as the signal will be subjected to severe loss. Thus the operation band should be chosen such that notches are avoided.

The transfer function is seen as a cascade of the amplitude responses for individual resonant circuits which correlates well with both the simulations and measurement results presented here. This is because of the multiple cascaded single resonant points along the cable as the signal propagates. In [5] an evolutionary strategy is employed to determine the optimized RLC component parameters of the resonant points for the SRC model, while in [3, 10] the transmission line equivalent SRC is employed to determine the values of the RLC component parameters. In this research, we employ the transmission line equivalent PRC to obtain the optimized values for the RLC component parameters.

It is worth noting that as the frequency and branch length increases, the signal amplitudes are consequently attenuated. This implies that attenuation in the power line channel is a factor of frequency and cable length.

4.6   Chapter Summary

In this chapter, the PLC channel has been characterized and studied as a transmission line composed of a cascade of parallel resonant circuits connected to a line of a known characteristic impedance. Based on this characterization, a PRC model is presented. Networks are built based on the model and measurements done for validation and results compared to the SRC model results. Results from the two models compare well and therefore the power line network has been successfully modelled as a communication channel using the PRC model. The PLC channel transfer function is observed to have notches whose position, depth and width are dependent on the branch length, load and characteristics of the power line studied in chapters 1 and 2.

Chapter 5

MEASUREMENTS AND MULTIPATH CHARACTERIZATION OF THE PLC CHANNEL

5.1   Introduction

The in-door low-voltage power line network allows for the building of an in-house telecommunication network in the most cost effective way in that no extra costs of installations are incurred. This is due to the ubiquitous network providing connectivity points in the houses and buildings connected to the grid [6], [16], [61], [72]. However, the power line network characteristics that include varying impedance, noise, attenuation, signal scattering and reflections due to numerous branching points, are the most unfavourable conditions for data transmission [21,32,33], the reason being that the power line network was designed for distribution of electrical energy [16]. These signal scattering characteristics in the PLC environment result in the receiver receiving a superposition of multiple attenuated and phase-shifted copies of the transmitted signal. This therefore calls for channel models, multipath and time variant characterization which play one of the most important roles in the design and analysis of PLC systems [6,7,65]. The common approach used in this research to investigate the multipath and time variant characteristic of the power line channel, is the extraction of multipath parameters from a large set of measurement data, a procedure which [46], [58], [73] and [74] have also used in their works among other researchers.

Even though multipath characterization of the in-door low-voltage PLC propagation channel has been performed and reported by several researchers, these reports are mainly based on simulated statistical characterization of the power line channel impulse response with few experimental results available [46]. Although characterization of the power line channel requires a comprehensive evaluation of its impulse response, characterization through the known channel multipath propagation parameters that include Root Mean Square (RMS) delay spread, mean excess delay and maximum excess delay spread have proved useful [46], [50], [51], [55], [75]. The work presented herein focuses on the analysis and characterization the PLC channel multipath and time-variant nature of the PLC channel using the above mentioned multipath propagation parameters in typical networks

with unknown network topologies and configurations through measurements. All these mentioned parameters are defined and discussed in the subsequent sections.

5.2   Multipath Propagation in PLC Channel

The power line channel is regarded as a multipath environment due to the multiple reflections of signals at impedance discontinuities resulting in transmitted signals reaching the receiver not only through the direct path but also through delayed and attenuated paths [5], [6], [50], [55]. To understand, analyse and characterize this multipath phenomenon, we resort to determining the multipath parameters that provide important information on the data transmission rates and dispersive characteristics of the power line channel [46,54,59]. As shown in Figure 5.1, the power line channel can be characterized as a linear time variant (LTV) system [59,75] with input, $x(t)$ and output, $y(t)$, assumed to comprise N discrete paths of propagation with each path having an amplitude attenuated by a factor α_k, a phase-shift θ_k, a propagation delay τ_k and noise factor $n(t)$ [5,75,76].
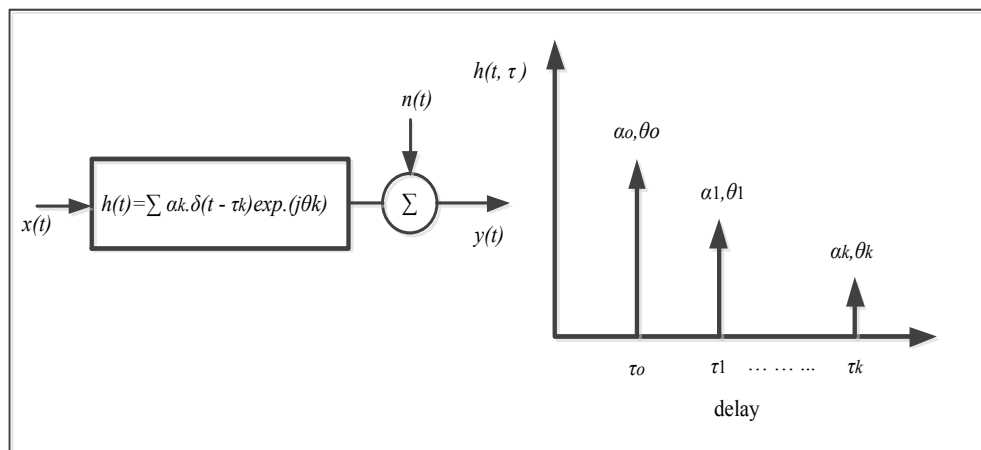
Figure 5.1: Mathematical model of the channel

Mathematically, the power line network channel impulse response can be represented as [5,75]:

$$h(t) = \sum_{k=1}^{N} \alpha_k \delta(t - \tau_k) e^{j\theta_k} \tag{5.1}$$

where $k = 1, 2, 3, \cdots, N$ is the number of paths, with δ being the Dirac delta function [5,75]. The phase-shift, θ_k is given as [5]:

$$\theta_k = \arctan\left(\frac{im\{\alpha_k\}}{Re\{\alpha_k\}}\right) \tag{5.2}$$

The impulse transfer function is composed of a sum of N Dirac delta pulses which are delayed by τ_k and have frequency dependent phase-shifts [5].

5.3 Measurement Set-up and Procedures

The complete measurement set-up and procedures are as presented in chapter 3. Extensive measurement of the channel transfer functions in the selected unknown network locations were done using the Rohde & Schwartz ZVL13 VNA in the frequency band of 10 KHz - 30 MHz. The lowest frequency of the VNA of 10 KHz, was set to ensure that our channel frequency responses included all frequencies up to 30 MHz.

5.4 Data Analysis and Channel Response Results

5.4.1 Channel Frequency Response (CFR)

We performed channel transfer measurements in the frequency domain through acquisition of the S_{21} parameter with a VNA from the various channels. From the basic definition of the channel frequency response as the ratio of the voltage at the receiver port of the VNA to the voltage at the transmit port of the VNA [58, 77], we denoted the S_{21} parameter as the channel frequency response $H(f)$, as shown in Figures 5.2, 5.3, 5.4, 5.5, 5.6 and 5.7.
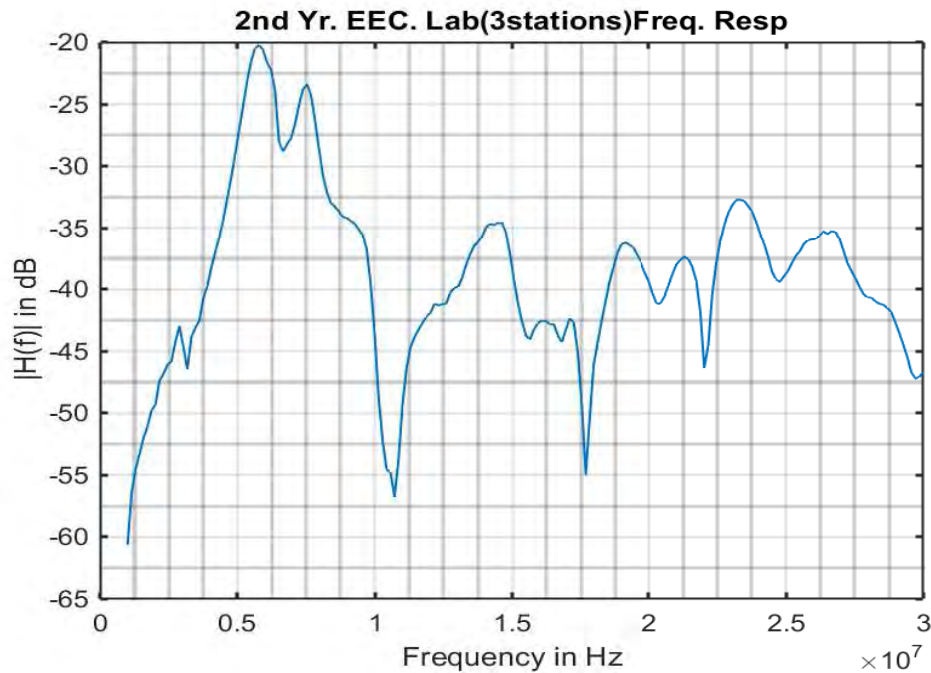
Figure 5.2: Frequency response profile for Second Year EEC Engineering laboratory (three workstations)

51
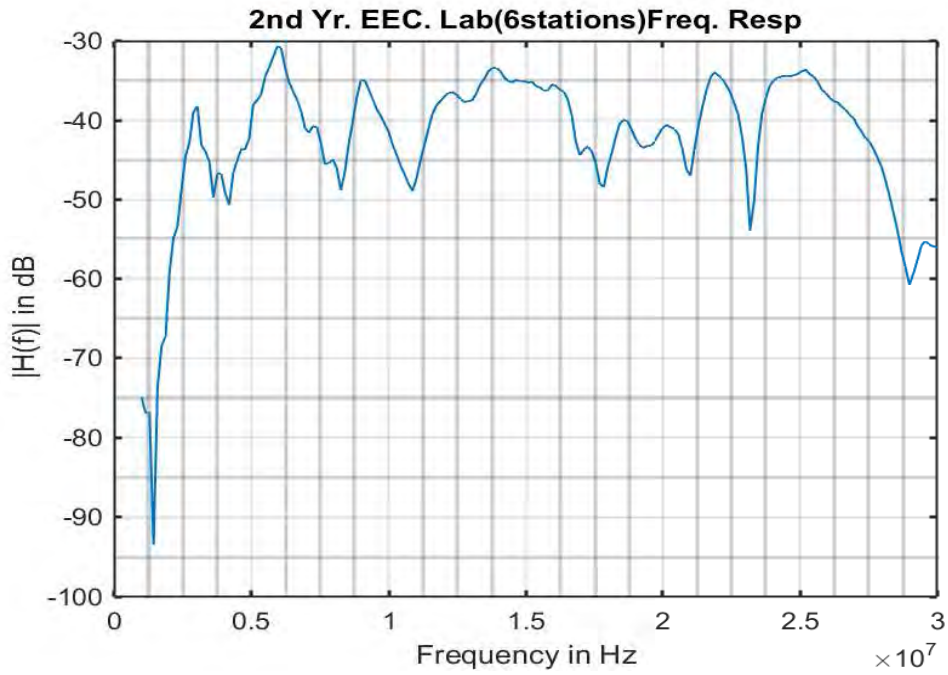
Figure 5.3: Frequency response profile for Second Year EEC Engineering laboratory (six workstations)
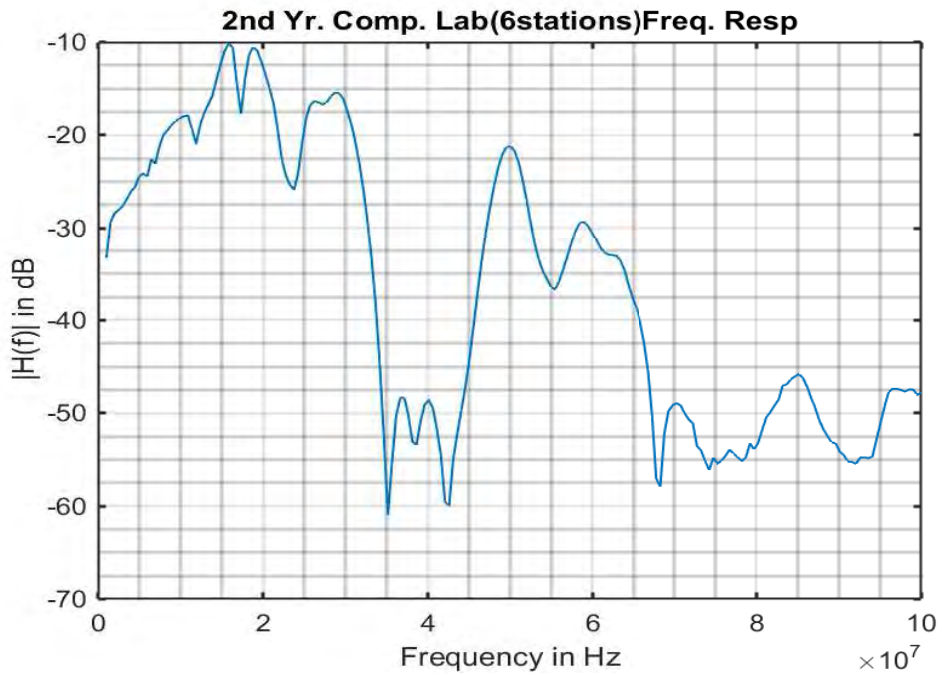
Figure 5.4: Frequency response profile for Second Year EEC Engineering computer laboratory (six workstations)
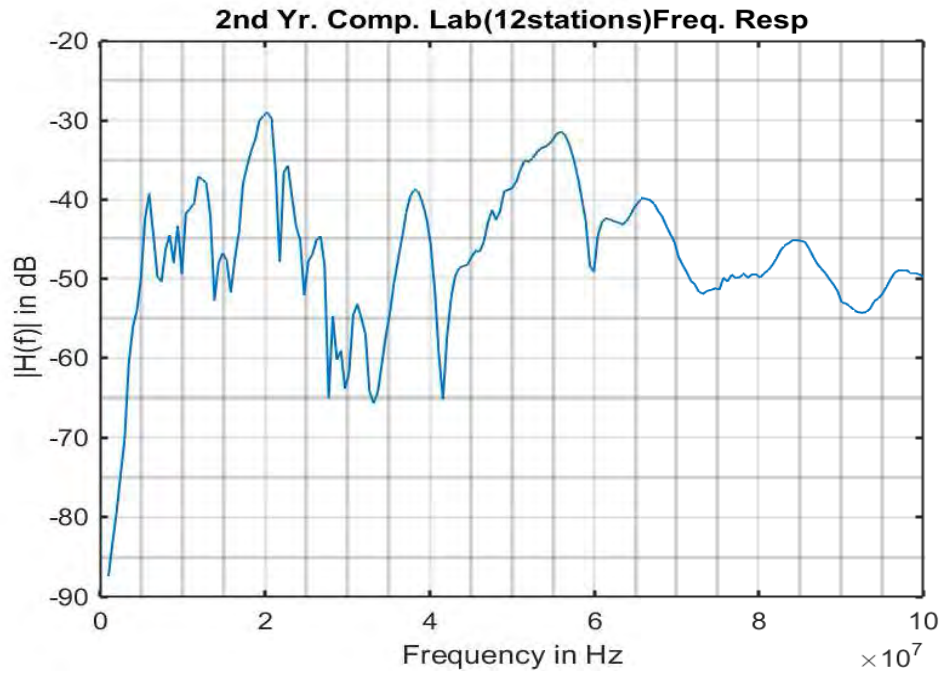
Figure 5.5: Frequency response profile for Second Year EEC Engineering computer laboratory (twelve workstations)
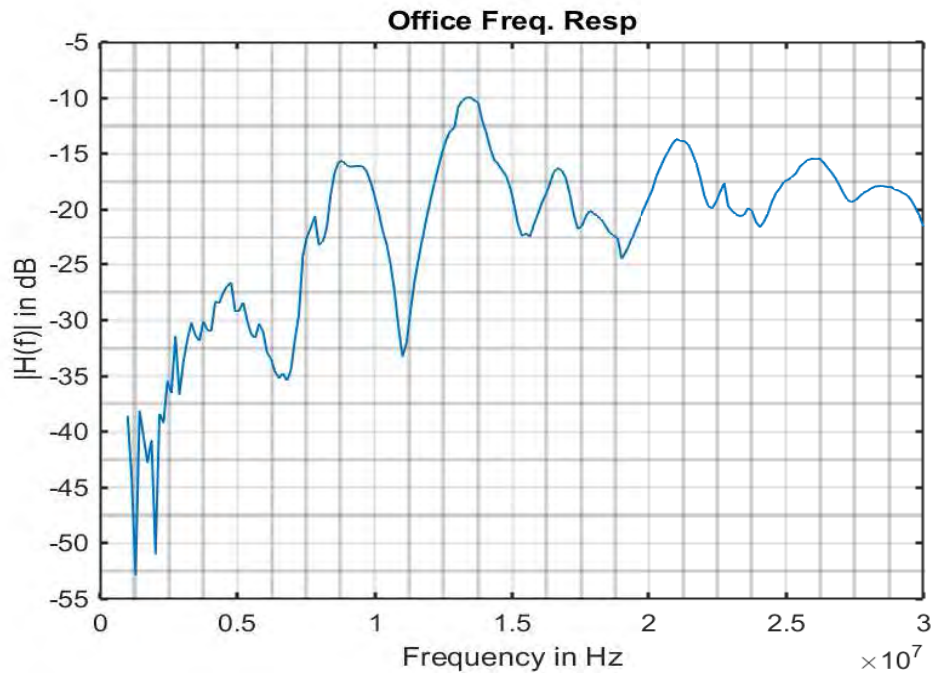
Figure 5.6: Frequency response profile for the office
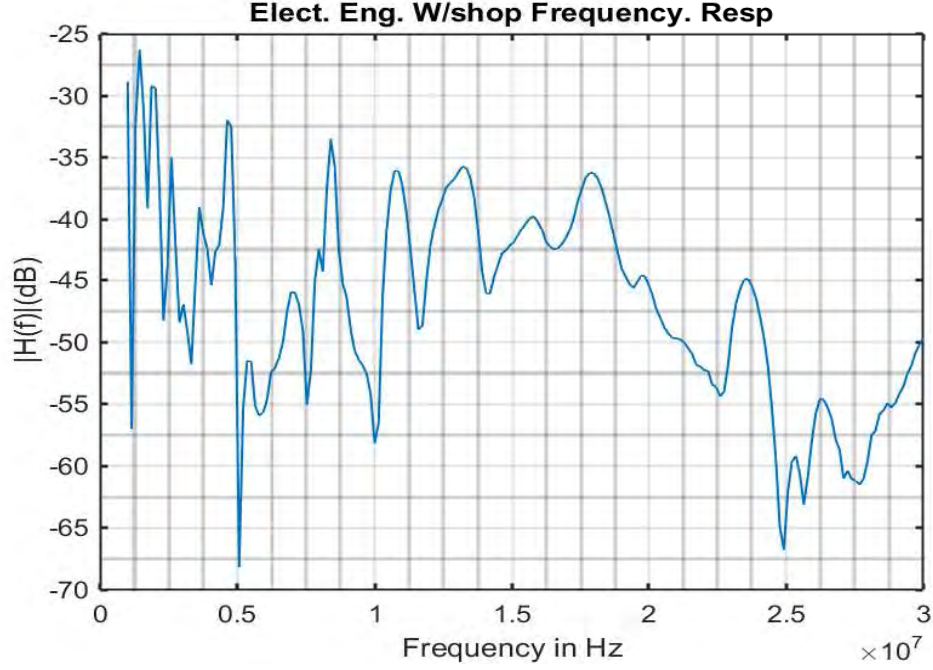
Figure 5.7: Frequency response profile for Electrical Engineering workshop

5.4.2 Channel Impulse Responses (CIR)

Because of our interest in the time-variant multipath characteristics of the channel, the measured channel transfer functions $H(f)$, were then transformed to the CIR, $h(t)$. This transformation was accomplished through the Inverse Discrete Fourier Transformation (IDFT) in Matlab. The following procedures was adopted with the term m referring to the frequency samples within the frequencies of $f_1 = 10$ KHz, and $f_2 = 30$ MHz:

- Windowing of the measured CFR data: Our focus on the CFR was in the frequency range from f_1 to f_2. The measured CFR were defined in the discrete frequency domains from f_1 to f_2. This resulted in a total of $m + 1$ discretized data samples.

- IDFT was then done to obtain the real CIR at time instant $t = rT$, where $r = 0, \cdots, R$, $R = 2m$, and T being the resolution in time. Thus the CIR was defined in discrete time domains with temporal resolution $\Delta t = 1/[(m + 1)\Delta f]$ with Δf being the resolution bandwidth.

- Each obtained CIR data were then normalized by their respective mean and standard deviations.

Figures 5.8, 5.9, 5.10, 5.11, 5.12, and 5.13 are the processed CIR results for all the locations.
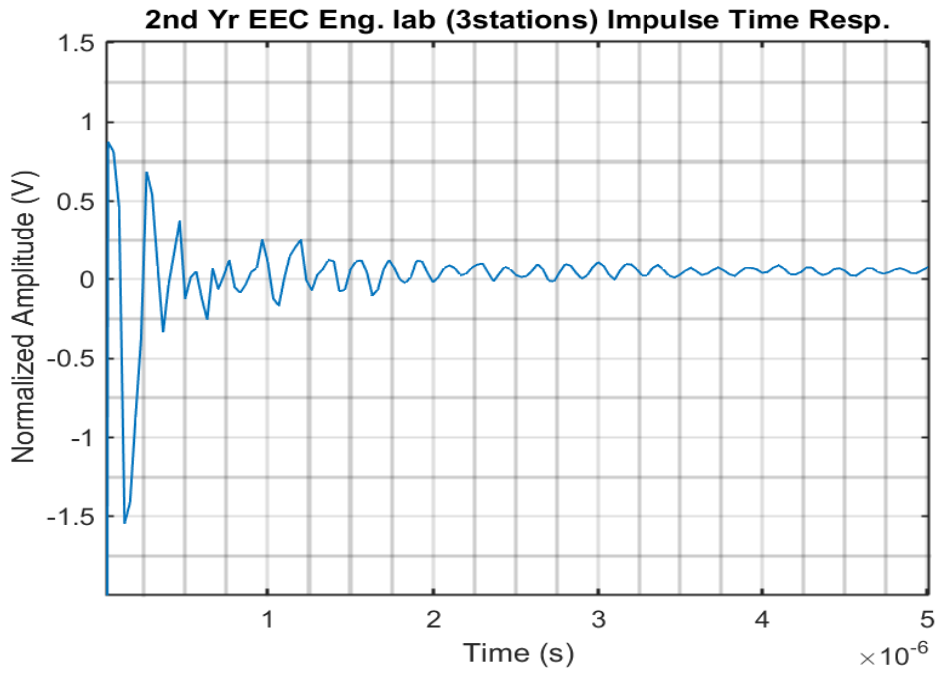
Figure 5.8: Impulse response profile for Second Year EEC Engineering laboratory (three workstations)
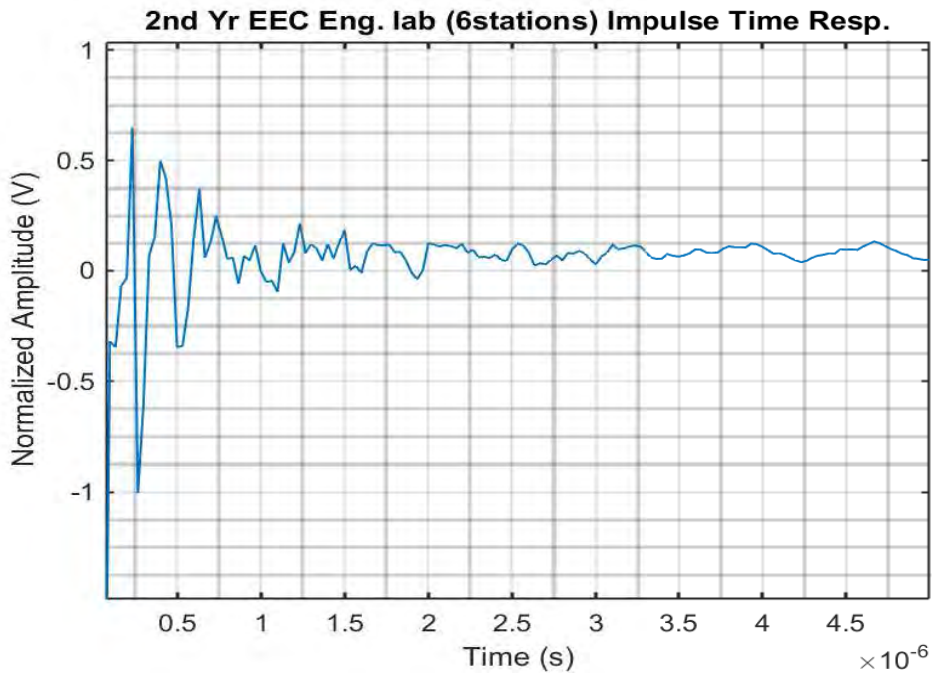
Figure 5.9: Impulse response profile for Second Year EEC Engineering laboratory (six workstations)
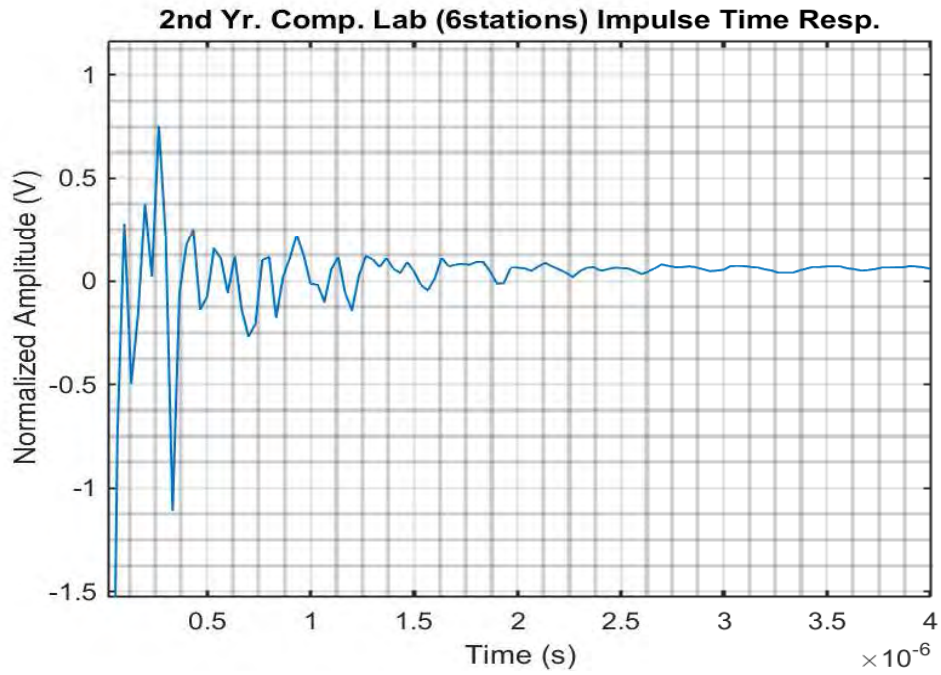
Figure 5.10: Impulse response profile for Second Year EEC Engineering computer laboratory (six workstations)
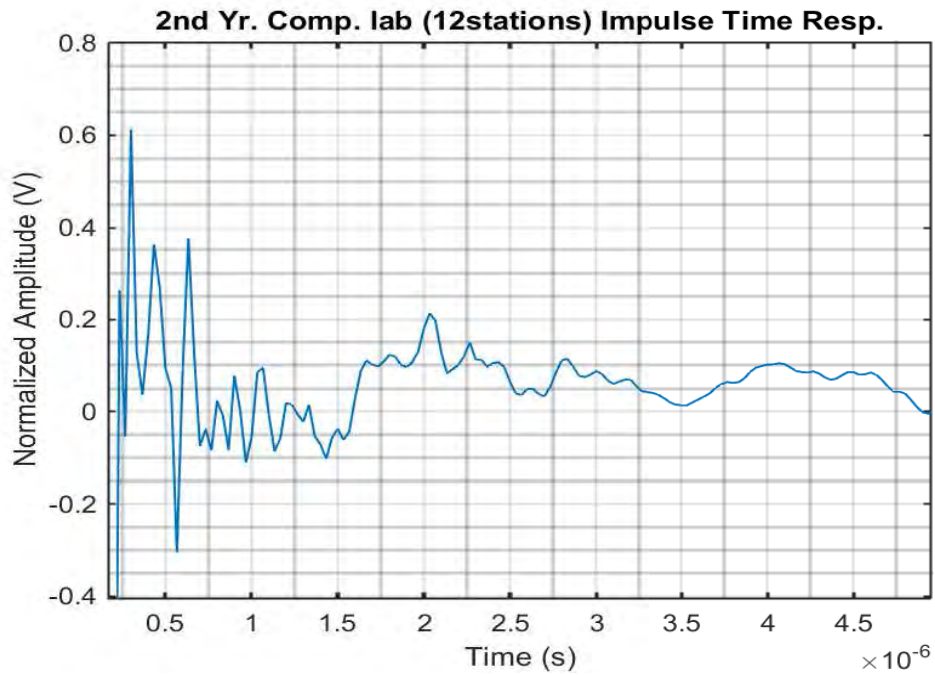
Figure 5.11: Impulse response profile for Second Year EEC Engineering computer laboratory (twelve workstations)
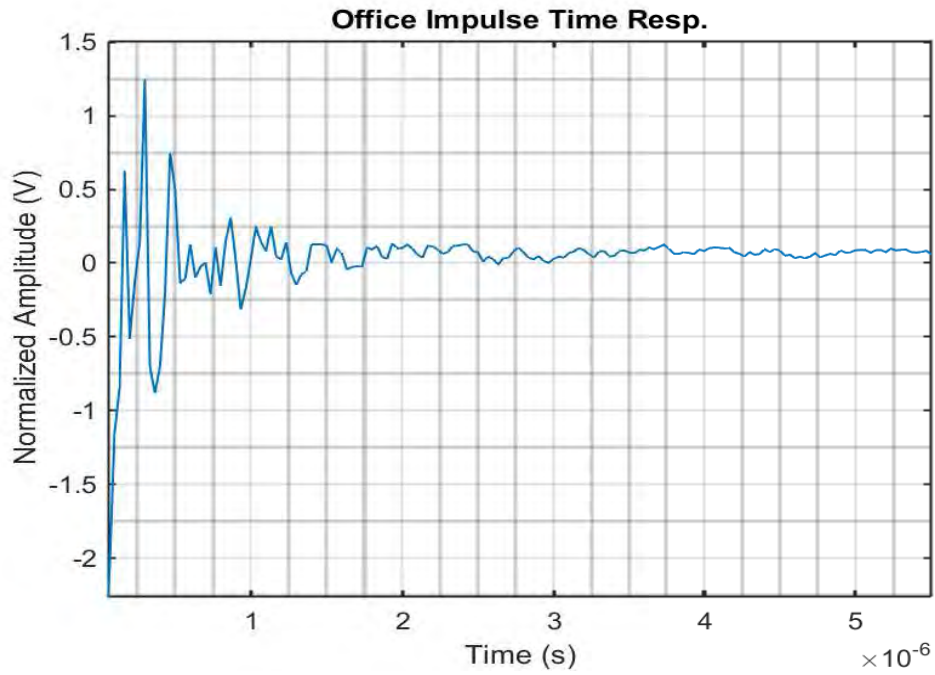
Figure 5.12: Impulse response profile for the office
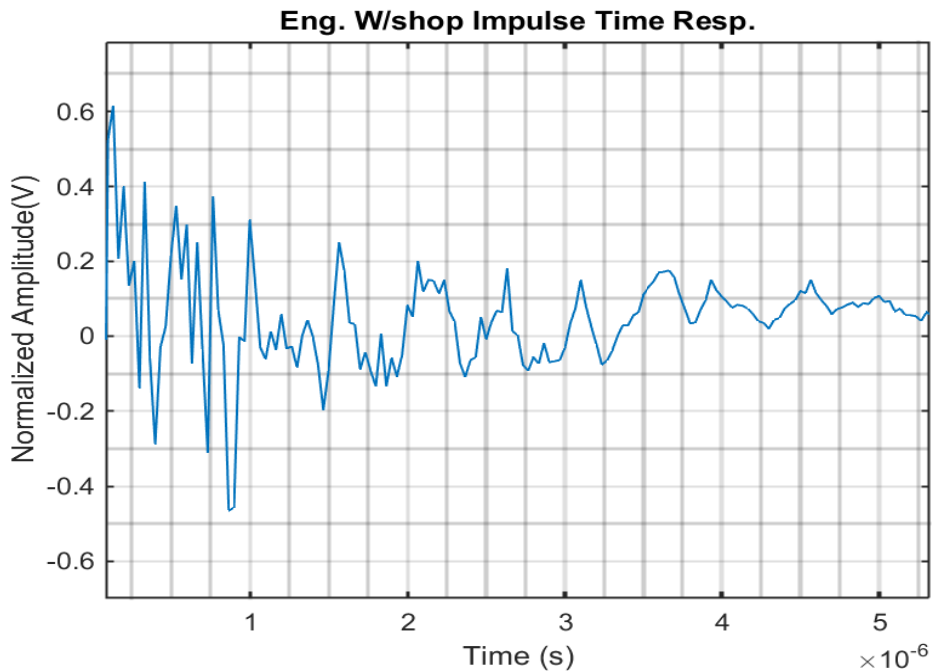
Figure 5.13: Impulse response profile for Electrical Engineering workshop

From these channel transfer functions, deep and narrow notches occur and are spread over the whole frequency range. These notches are due to the multiple reflections at the points of discontinuities and impedance mismatches. In addition, the length of the impulse responses and the number of the peaks that occur, vary considerably and depend on the network topology, terminal loading profiles and the environment.

5.5 Multipath Propagation Parameters

In order to compare different multipath channels and develop general guidelines for PLC systems, multipath parameters are used to quantify the multipath and time variant channel [49,60,76]. Next, the key multipath and time variant parameters that include: mean excess delay, RMS delay spread and maximum excess delay spread are discussed. In addition, the relationship between the coherence bandwidth and the RMS delay spread of the networks is also studied statistically.

5.5.1 Mean Excess Delay $(\bar{\tau}_e)$

This is the first moment of the power delay profile and is given by [75,76]:

$$\bar{\tau}_e = \frac{\sum_k a_k^2 \tau_k}{\sum_k a_k^2} = \frac{\sum_k P(\tau_k)\tau_k}{\sum_k P(\tau_k)} \tag{5.3}$$

where τ_k, a_k, and $k = 1, 2, 3, \cdots$, are the signal arrival delay, amplitude of delay arrival and delay position respectively in the received power delay profile, while the power delay profile is defined as $P(\tau_k) = |h(\tau)|^2 / \int_0^\infty |h(\tau)|^2 d\tau$ [60, 75, 76].

5.5.2 Root Mean Square (RMS) Delay Spread (τ_{rms})

This is the square root of the second central moment of the power delay profile. It gives an account for the energy dispersion in the impulse response of the channel [59]. It is defined by [76]:

$$\tau_{rms} = \sqrt{\bar{\tau^2} - \bar{\tau}_e^2} \tag{5.4}$$

Where $\bar{\tau^2}$ is the second moment of the power delay profile given as:

$$\bar{\tau^2} = \frac{\sum_k a_k^2 \tau_k^2}{\sum_k a_k^2} = \frac{\sum_k P(\tau_k)\tau_k^2}{\sum_k P(\tau_k)} \tag{5.5}$$

These delays are measured relative to the first arriving signal at the receiver at delay $\tau_0 = 0$. Equations (5.3) and (5.4) rely only on the relative amplitudes of the multipath components within $P(\tau_k)$ [49, 60, 76].

5.5.3 Maximum Excess Delay Spread (τ_X)

Maximum excess delay, is defined to be the time delay during which the multipath energy falls to X dB below the maximum in the power delay profile. It is defined by $\tau_X - \tau_0$, where τ_0 refers to the first arriving signal and τ_X is the maximum delay at which a multipath component is within X dB of the arriving multipath component with the highest amplitude and does not necessarily arrive at τ_0 [49, 60, 76].

Maximum excess delay defines the temporal extent of the multipath that is above a particular threshold [44], [45]. In this work, the noise floor threshold was set at 0.125 V in the $h(t)$ graph delay profiles to differentiate between received multipath components and noise.

Table 5.1 shows the statistics of the extracted multipath parameters from the various CIR delay profiles.

Table 5.1: Statistics of the extracted multipath delay parameters

Locations	Parameters (μs)			
	τ_o	$\bar{\tau}_e$	τ^2	τ_{rms}
EEC Eng. lab.(3stns)	0.031	0.233	0.067	0.113
EEC Eng. lab.(6stns)	0.250	0.451	0.245	0.204
Computer. lab.(6stns)	0.094	0.267	0.075	0.058
Computer. lab.(12stns)	0.250	0.540	0.307	0.124
Office	0.125	0.373	0.150	0.104
Workshop	0.063	0.754	2.035	1.211

It is important to note that the RMS delay spread and mean excess delays are defined from a single power delay profile that is a temporal average of consecutive impulse response measurements collected and averaged over a local area.

5.6 Coherence bandwidth (B_c)

While the RMS delay spread is a natural quantity caused by the reflected and scattered propagation paths in the power line network channel, the coherence bandwidth, (B_c), is a relation derived statistically from the RMS delay spread. Coherence bandwidth is used as a statistical measure of the frequency band within which the channel can be considered "flat". This means the spectral components within this range of frequencies have approximately equal gain and linear phase. Coherence bandwidth is defined in terms of correlation function of the frequency response ($R(\psi)$), given as (5.6) [8,73]. It measures the correlation magnitude between the channel response between two spaced frequencies.

$$R(\psi) = \int_{-\infty}^{\infty} H(f)H^*(f + \psi)df \qquad (5.6)$$

where ψ is the frequency shift and * refers to the complex conjugate. Table 5.2 shows the computed coherence bandwidths based on 0.5 and 0.9 correlation levels

Table 5.2: Coherence bandwidth values for 0.5 and 0.9 correlation levels

Locations	Parameters	
	$B_{0.5}$	$B_{0.9}$
EEC lab.(3stns)	1.770 MHz	176.991 KHz
EEC lab.(6stns)	0.980 MHz	98.039 KHz
Comp. lab.(6stns)	3.448 MHz	344.828 KHz
Comp. lab.(12stns)	1.613 MHz	161.290 KHz
Office	1.923 MHz	192.308 KHz
Workshop	0.166 MHz	16.515 KHz

5.7 Discussion of Results

Based on measurement results, we defined the complexity of the networks based on the different terminal loading conditions and circuit connections at the distribution boards. A circuit running from and to the same circuit breaker at the distribution board were considered single networks, while the circuits that terminated at different circuit breakers were considered to form parallel connected networks.

From inspection of Table 5.2, a clear and consistent dependence of the RMS delay spread on the loading conditions of the different power supply networks in the different locations were noted. The RMS delay spread values increased with increased loading profiles in the different power supply networks, and hence a reduction in the coherence bandwidths. This reduction in bandwidth witnessed is not a favourable condition for broadband data transmission and thus very suitable coding and modulation schemes are called for to mitigate against such conditions in PLC.

The dependence of the delay spread on the network topology and configuration is an important observation in this study that would thus greatly influence PLC system design. A review results obtained in previous works shows good agreement. In this regard, the results obtained here, were compared to results reported for a single postgraduate office from UKZN (1 - 30 MHz), USA (1.8 - 30 MHz) and for frequency band A (1.7 - 30 MHz) from France as presented in [46], [56] and [57] respectively among other researchers as shown in Table 5.3.

Table 5.3: Comparison of RMS delay spread values

Parameters(μsec)	UKZN	UKZN [46]	USA [56]	France [57]
Minimum	0.058	0.022	0.090	0.026
Maximum	1.211	1.160	1.810	1.039
Mean	0.302	0.287	0.530	0.309
Standard dev.	0.448	0.222	0.290	0.212

From Table 5.3, our minimum and maximum delay spread values of $0.058\mu s$ and $1.211\mu s$ were observed to be comparable to others. In addition, our mean RMS delay value of $0.302\mu s$ compared very well with $0.287\mu s$ which was reported previously from UKZN in [46]. However, our mean RMS delay value was lower than $0.530\mu s$ and $0.309\mu s$

reported in [56] and [57]. These variations can be attributed to the different terminal loading conditions and different network topologies at all the locations. In addition, our standard deviation of $0.448\mu s$ was higher than other results. This actually shows the amount of spread out in our RMS delay spread results between the maximum and minimum values which corresponds to the complexity of the networks in the different selected locations.

5.8   Chapter Summary

In this Chapter, measurements and analysis of the multipath characteristics of the power line network channel for selected locations within the University of KwaZulu-Natal were investigated and presented. From the analysis, it is evident that the power line channel is a time varying channel due to the ever varying channel impedance, mismatched branching points, and terminal load impedances causing scattering in the transmitted signal, thus leading to multipath fading propagation. In addition, we have also compared our mean delay with results from other regions employing a similar approach and found the results to be in good agreement with them.

Chapter 6

CONCLUSIONS AND FUTURE WORK

With the ever increasing demand for high speed and broadband data communication with increasing cost of installing new infrastructure, PLC offers the best alternative cost-free infrastructure. It is therefore a necessity to have accurate channel models that form the basis for computer based simulations and measurements. Furthermore, a comprehensive knowledge and understanding of the channel characteristics is very important since the PLC channel is a harsh and unpredictable environment.

In this dissertation, a comprehensive measurement plan and procedure is outlined and a review of the fundamental bottom-up and top-down modelling approaches presented for different domains. Then, using the bottom-up approach, a PRC model based on a two-wire transmission line theory is presented with analysis and measurements done in the frequency domain. Also, in the top-down approach, analysis of the multipath propagation characteristics is done in the time domain to study the multipath and time variant nature of the power line network from typical power line networks. From the results obtained, all research objectives outlined in the first chapter were attained.

6.1   Summary of Results

- Through design, simulation and measurements in the frequency band of 1-30 MHz, the power line network was successfully modelled as a communication channel based on a PRC model in chapter 4. This model was based on the well-known two-wire transmission line theory. The model was validated under different network configurations built in the PLC laboratory within the University of KwaZulu-Natal. The PRC model results were also compared to the SCR model presented in [3,10] and results found to match well. Further investigations on the effects of varying branch lengths in the different network configurations on the channel transfer functions were done. From this variation in branch lengths, the following observations were made: shorter branch cables had very wide and deep notches than longer branch cables, having branch cables of same lengths in succession resulted into wide and deep notches and long branch cables had the highest level of signal attenuation. These conditions could result in partial or total loss of data packets during transmission. With these information, very robust coding and modulation schemes could then be designed and implemented to mitigate against such catastrophic sources of losses in

a PLC system.

- In chapter 5, we have investigated the PLC channel time variant and multipath characteristics from a set of measurement data collected from selected locations within the University of KwaZulu-Natal in the frequency band of 10 KHz - 30 MHz. We then analysed the effects of the network characteristics and loading profiles on the received signal and established that the RMS delay spread increased with increasing loading profile of the network topology but inversely to the coherence bandwidth. The results obtained were compared to other results obtained using similar approach and a previous result from one office from the University of KwaZulu-Natal. We achieved results that were very comparable to others, with an assumption of network topologies and methods used in processing their measurement data.

6.2 Future Work

In this dissertation, it is seen that extensive channel transfer function measurements inform the prediction of the channel behaviour and mean delay response. From this knowledge, this dissertation can be extended through further research in PLC as follows:

- From the channel impulse response results presented, a dominant line of sight (LOS) signal is observed at the receiver with several other late arriving signals of low amplitudes. This is an attenuation characteristic of the PLC channel, which is a factor of cable length and frequency of transmission. Therefore, in this regard, further work is proposed to determine statistical models that can well describe the average PLC channel attenuation.

- In this research, we have employed the conventional method of indirectly characterizing signal propagation delay in the PLC channel through channel impulse responses. This may not fully address the most important delays that occur due to multiple retransmission of lost data in a noisy PLC environment. As a consequence, data delay sensitive applications may not be properly realized. We therefore propose further work on finding an efficient data delay measurement accompanied with a high level statistical modelling approach.

- From the mean delay spread results obtained, we propose further investigation on the design and evaluation of possible and suitable robust coding and modulation schemes for realization of a prototype modem.

References

[1] M. N. O. Sadiku, *Elements of Electromagnetics*. Oxford University Press, second ed., 1995.

[2] D. M. Pozar, *Microwave Engineering*. John Wiley & Sons Inc., second ed., 1998.

[3] F. Zwane, *Power Line Communication Channel Modelling*. MSc. Dissertation, Durban, South Africa: University of KwaZulu-Natal, 2014.

[4] http://www.testequipmentdepot.com/rohdeschwarz/pdf/zvl13_data.pdf, Accessed: May 10 2015.

[5] H. Philips, "Modelling of power line communication channels," in *Proceedings of Int. Symposium on Power-Line Communications and Its Application (ISPLC)*, Vancouver, Canada, pp. 14–21, 6-8, Apr. 2005.

[6] M. Zimmermann and K. Dostert, "A multipath model for the power line channel," *IEEE Trans. On Commun.*, vol. 50, no. 4, pp. 553–559, Apr. 2002.

[7] J. Anatory and N. Theethayi, *Broadband Power-Line Communication Systems: Theory and Applications*. WIT Press, 2010.

[8] M. Mosalaosi, *Power Line Communication (PLC) Channel Measurements and Characterization*. MSc. Dissertation, Durban, South Africa: University of KwaZulu-Natal, 2014.

[9] D. K. Misra, *Radio-Frequency and Microwave Communication Circuits: Analysis and Design*. John Wiley & Sons, Inc., 2001.

[10] F. Zwane and T. J. O. Afullo, "An alternative approach in power line communication channel modelling," *Progress In Electromagnetics Research C*, vol. 47, pp. 85–93, 2014.

[11] M. Arzbergerl, K. Dostert, T. Waldeck, and M. Zimmermann, "Fundamental properties of the low voltage power distribution grid," in *Proceedings of IEEE Int. Symposium on Power-Line Communications and Its Applications(ISPLC)*, Essen, Germany, pp. 45–50, 2-4, Apr. 1997.

[12] A. Hosemann, "PLC applications in low voltage distribution networks," in *Proceedings of IEEE Int. Symposium on Power-Line Communications and Its Applications(ISPLC)*, Essen, Germany, pp. 134–139, 2-4, Apr. 1997.

[13] H. Hrasnica, A. Haidine, and R. Lehnert, *Broadband Power Line Communications Networks, Network Design*. John Wiley & Sons Ltd, 2004.

[14] K. S. A. Mawali, *Techniques for Broadband Power Line Communications: Impulsive Noise Mitigation and Adaptive Modulation.* PhD Thesis, Melbourne, Australia: RMIT University, July 2011.

[15] T. Waldeck, M. Busser, and K. Dostert, "Telecommunication applications over the low voltage power distribution grid," in *Proceedings of IEEE 5th Int. Symposium on Spread Spectrum Techniques and Application*, Sun City, South Africa, pp. 73–77, 2-4, Sep. 1998.

[16] S. O. Awino and T. J. O. Afullo, "Power line communication channel modelling using parallel resonant circuits approach," in *Proceedings of South Africa Telecommunication Networks and Applications Conference (SATNAC)*, Western Cape, South Africa, pp. 353–357, 6-9, Sep. 2015.

[17] *An American National Standard IEEE Guide for Power-Line Carrier Applications, ANSI/IEEE Std. 643-1980, Approved*, March 15 1979.

[18] J. Onunga and R. W. Donaldson, "Power line communication using CSMA access control with priority acknowledgement," *IEEE Trans. On Power delivery*, vol. 4, no. 2, pp. 878–886, Apr. 1989.

[19] M. Tanaka, "Transmission characteristics of a power line used for data communications at high frequencies," *IEEE Trans. on Consumer Electronics*, vol. 35, no. 1, pp. 37–42, 1989.

[20] R. M. Vines, H. J. Trussell, L. J. Gale, and J. J. Ben O'Neal, "Noise on residential power distribution circuits," *IEEE Trans. On Electromagn. Comp.*, vol. EMC-26, no. 4, pp. 161–168, Nov. 1984.

[21] M. Tanaka, "High frequency noise power spectrum, impedance and transmission loss of power line in japan on intrabuilding power line communications," *IEEE Trans. On Consumer Electronics*, vol. 34, no. 2, pp. 321–326, May 1988.

[22] M. H. Shwehdi and A. Z. Khan, "A power line data communication interface using spread spectrum technology in home automation," *IEEE Trans. On Power Delivery*, vol. 11, no. 3, pp. 1232–1237, Jul. 1996.

[23] C. J. Kim and M. F. Chouikha, "Attenuation characteristics of high rate home-networking PLC signals," *IEEE Trans. On Power Delivery*, vol. 17, no. 4, pp. 945–950, Oct. 2002.

[24] J. D. Glover, M. S. Sarma, and T. J. Overbye, *Power System Analysis and Design.* Cengage Learning, fifth ed., 2012.

[25] T. Gonen, *Electric Power Transmission System Engineering: Analysis and Design.* CRC Press, second ed., 2008.

[26] R. M. Vines, H. J. Trussel, K. C. Shuey, and J. J. B. O'Neal, "Impedance of the residential power-distribution circuit," *IEEE Trans. Electromagn. Compat.*, vol. EMC-27, pp. 6–12, Feb. 1985.

[27] H. Philips, "Performance measurements of power line channels at high frequencies," in *Proceedings of Int. Symposium on Power-Line Communications and Its Application (ISPLC)*, Tokyo, Japan, pp. 229–237, 24-26, Mar. 1998.

[28] D. Liu, E. Flint, B. Gaucher, and arid Y. Kwarket, "Wide band AC power line characterization," *IEEE Trans. On Consumer Electronics*, vol. 45, pp. 1087–1097, Nov. 1999.

[29] F. Zwane and T. J. O. Afullo, "Power line communication channel modelling: Establishing the channel characteristics," in *Proceedings of South African Universities Power Engineering Conference (SAUPEC)*, Durban, South Africa, 30-31, Jan. 2014.

[30] J. Anatory, N. Theethayi, R. Thottappillil, M. Kissaka, and N.H.Mvungi, "The effects of interconnections and branched network in the broadband power line communications," in *Proceedings of Int. Union of Radio Science (URSI) Assembly*, New Delhi, Oct. 2005.

[31] W. Cai, J. Le, and K. pei Liu, "The analysis of the in-door PLC channel characteristics based on information nodes channel modelling method," *Int. Journal of Computer and Electrical Engineering*, vol. 5, no. 2, pp. 155–159, Apr. 2013.

[32] H. Meng, Y. L. Guan, and S. Chen, "Modelling and analysis of noise effects on broadband power line communications," *IEEE Trans. On Power Delivery*, vol. 20, no. 2, pp. 630–637, Apr. 2005.

[33] M. Zimmermann and K. Dostert, "Analysis and modelling of impulsive noise in broadband power line communications," *IEEE Trans. On Electromagn. Comp.*, vol. 44, no. 1, pp. 249–258, Feb. 2002.

[34] L. A. Berry, "Understanding middleton's canonical formula for class A noise," *IEEE Trans. On Electromagn. Comp.*, vol. EMC-23, no. 4, pp. 337–344, Nov. 1981.

[35] *Standard Specifications for Electrical Installation and Electrical Equipment.* http://www.publicworks.gov.za/PDFs/consultants_docs/ELECMECHSERVICES.PDF, South Africa.

[36] Y.-S. Kim and J.-C. Kim, "Characteristic impedance in low-voltage distribution sytems for power line communication," *Journal of Electrical Engineering & Technology*, vol. 2, no. 1, pp. 29–34, 2007.

[37] M. Gotz, M. Rapp, and K. Dostert, "Power line channel characteristics and their effect on communication systems design," *IEEE Trans. On Commun.*, vol. 42, no. 4, pp. 78–86, Apr. 2004.

[38] M. Zimmermann and K. Dostert, "An analysis of the broadband noise scenario in power line networks," in *Proceedings of Int. Symposium on Power-Line Communications and Its Application (ISPLC)*, Limerick, Ireland, pp. 131–138, 5-7, Apr. 2000.

[39] P. Strong, "Regulatory & consumer acceptance of power line products," in *Proceedings of the 5th Int. Symposium on Power-Line Communications and its Applications (ISPLC'01)*, Malmo, Sweden, pp. 175–184, Apr. 2001.

[40] *European Telecommunications Standards Institute (ETSI)*. www.etsi.org/WebSite/Technologies/Powerline.aspx.

[41] *IEEE P1901, Draft Standard for Broadband over Power Line Networks: Medium Access Control and Physical Layer Specifications, PUA and UPA contribution to IEEE 1901 call for submission on BPL access requirements Functional and Technical Requirements.* www.upaplc.org, Feb. 2006.

[42] D. Shaver, *Low Frequency, Narrowband PLC Standards for Smart Grid–The PLC Standards Gap.* Texas Instruments Incorporated, http://cms.comsoc.org/SiteGen/Uploads/Public/Docs_Globecom_2009/6_-_12-03-09_shaver_smart_grid_panel_final.pdf, Dec. 3 2009.

[43] *ITU Approved Standards for Smart Grid: Recommendations ITU-T G.9955 and G.9956.* https://www.itu.int/net/pressoffice/press_releases/2011/CM16.aspx.

[44] A. Ndjiongue, A. Snyders, H. C. Ferreira, and S. Rimer, "Review of power line communications standards in Africa," in *Proceedings of 5th Int. Conference, AFRICOM*, Blantyre, Malawi, pp. 12–21, 25-27, Nov. 2013.

[45] T. A. Papadopoulos, C. G. Kaloudas, A. I. Chrysochos, and G. K. Papagiannis, "Application of narrowband power line communication in medium-voltage smart distribution grids," *IEEE Trans. On Power delivery*, vol. 28, no. 2, pp. 981–988, Apr. 2013.

[46] M. Mosalaosi and T. J. O. Afullo, "Dispersive characteristics for broadband indoor power line communication channels," in *Proceedings of South Africa Telecommunication Networks and Applications Conference (SATNAC)*, Nelson Mandela Bay, Eastern Cape, South Africa, pp. 313–317, 31 Aug.-3 Sep. 2014.

[47] R. E. Collin, *Foundations for Microwave Engineering.* John Wiley & Son, Inc., second ed., 2001.

[48] C. K. Alexander and M. N. O. Sadiku, *Fundamental of Electric Circuits.* McGraw-Hill, fourth ed., 2009.

[49] A. F. Molisch, *Wireless Communications.* Wiley-IEEE Press, second ed., 2011.

[50] D. Anastasiadou and T. Antanakopoulos, "Multipath characterization of in-door power line networks," *IEEE Trans. On Power Delivery*, vol. 20, no. 1, pp. 90–99, Jan. 2005.

[51] L. Liu, T. Cheng, and L. Yanan, "Analysis and modelling of multipath for indoor power line channel," in *Proceedings of IEEE Conference on Advanced Communication Technology*, Phoenix Park, Korea, 17-20, Feb. 2008.

[52] M. O. Asiyo and T. J. O. Afullo, "Power line communications channel multipath phenomena and rms delay spread," in *Proceedings of South Africa Telecommunication Networks and Applications Conference (SATNAC)*, Western Cape, South Africa, pp. 93–97, 6-9, Sep. 2015.

[53] S. Guzelgoz, H. B. Celebi, and H. Arslam, "Statistical characterization of the paths in multipath PLC channels," *IEEE Trans. On Power Delivery*, vol. 26, no. 1, pp. 181–187, Jan. 2011.

[54] H. Li, Z. Bi, D. Liu, J. Li, and P. Stoica, "Channel order and rms delay spread estimation for AC power line communications," in *Proceedings of the Tenth IEEE Workshop on Statistical Signal and Array Processing*, Pennsylvania, USA, pp. 229–233, 14-16, Aug. 2000.

[55] G. Huang, D. Akopian, and C. L. P. Chen, "Measurement and characterization of channel delays for broadband power line communications," *IEEE Trans. On Instrumentation and Measurements*, vol. 63, no. 11, pp. 2583–2590, Nov. 2014.

[56] S. Galli, "A simplified model for the indoor power line channel," in *Proceedings of IEEE Int. Symposium on Power-Line Communications and Its Applications (ISPLC)*, Dresden, Germany, pp. 13–19, 29 Mar.-1 Apr. 2009.

[57] T. R. Oliveira, C. B. Zeller, S. L. Netto, and M. V. Ribeiro, "Statistical modelling of the average channel gain and delay spread in in-home PLC channels," in *Proceedings of IEEE Int. Symposium on Power-Line Communications and Its Applications(ISPLC)*, Austin, Texas, USA, pp. 184–188, 29 Mar.-1 Apr. 2015.

[58] F. Versolatto and A. M. Tonello, "PLC channel characterization up to 300 MHz: Frequency response and line impedance," in *Proceedings of IEEE Global Telecommunications Conference (GLOBECOM)*, Anaheim, California, USA, pp. 3525–3530, 3-7, Dec. 2012.

[59] A. M. Tonello, F. Versolatto, and A. Pittolo, "In-home power line communication channel: Statistical characterization," *IEEE Trans. On Commun.*, vol. 62, no. 6, pp. 2096–2106, Jun. 2014.

[60] U. Madhow, *Fundamentals of Digital Communication*. Cambridge University Press, 2008.

[61] J. Anatory, N. Theethayi, M. M. Kissaka, and N. H. Mvungi, "Broadband power line communications: Performance analysis," *World Academy of Science, Engineering and Technology*, pp. 832–836, 24 2008.

[62] P. A. J. V. Rensburg and H. C. Ferreira, "Design of a bidirectional impedance-adapting transformer coupling circuit for low-voltage power line communications," *IEEE Trans. On Power delivery*, vol. 20, no. 1, pp. 60–70, Jan. 2005.

[63] S. S. Ali, A. Bhattacharya, and D. R. Poddar, "Design of bidirectional coupling circuit for broadband power line communications," *Journal of Electromagnetic Analysis and Applications*, vol. 4, pp. 162–166, 2012.

[64] L. Qi, S. Jingzhao, and F. Zhenghe, "Adaptive impedance matching in power line communication," in *Proceedings of Int. Conference on Microwave and Millimetre Wave Technology*, Nanjing, China, pp. 887–890, 18-21, Aug. 2004.

[65] M. P. Sibanda, P. A. J. V. Rensburg, and H. C. Ferreira, "Impedance matching with low-cost, passive components for narrowband PLC," in *Proceedings of IEEE Int. Symposium on Power-Line Communications and Its Applications (ISPLC)*, Udine, Italy, pp. 335–340, 3-6, April 2011.

[66] P. A. J. V. Rensburg, H. C. Ferreira, and A. J. Snyders, "Coupler winding ratio selection for effective power transfer to a power line communications receiver," in *Proceedings of IEEE Int. Symposium on Power-Line Communications and Its Applications (ISPLC)*, Orlando, USA, pp. 290–295, 26-29, March 2006.

[67] N. L. Zaw, H. A. Kyaw, and K. Z. Ye, "Power line cable transfer function for the broadband power line communication channel," *Universal Journal of Control and Automation*, vol. 1, no. 4, pp. 103–110, 2013.

[68] P. Mlynek, J. Misurec, M. Koutny, and R. Fujdiak, "Transfer function of power line channel-influence of topology parameters and power line topology estimation," in *Proceedings of IEEE PES Innovative Smart Grid Technologies Conference*, Istanbul, pp. 1–5, 12-15, Oct. 2014.

[69] A. B. Dalby, "Signal transmission on power lines: Analysis of power line circuits," in *Proceedings of IEEE Int. Symposium on Power-Line Communications and Its Applications(ISPLC)*, Essen Germany, pp. 37–44, 2-4, Apr. 1997.

[70] A. K. Mandal, *Introduction to Control Engineering: Modelling, Analysis and Design*. New Age Int., 2006.

[71] N. S. Nise, *Control Systems Engineering*. John Wiley & Sons, Inc., fourth ed., 2004.

[72] A. M. Nyete, T. J. O. Afullo, and I. Davidson, "On rayleigh approximation of the multipath PLC channel: Broadband through the PLC channel," in *Proceedings of South Africa Telecommunication Networks and Applications Conference (SATNAC)*, Nelson Mandela Bay, Eastern Cape, South Africa, pp. 265–270, 31 Aug.-3 Sep. 2014.

[73] H. Gassara, F. Rouissi, and A. Ghazel, "Statistical characterization of the indoor low-voltage narrowband power line communication channel," *IEEE Trans. On Electromagn. Comp.*, vol. 56, no. 1, pp. 123–131, Feb 2014.

[74] M. Tlich, A. Zeddam, F. Moulin, and F. Gauthier, "In-door power line communications channel characterization up to 100 MHz-part II: Time-frequency analysis," *IEEE Trans. On Power Delivery*, vol. 23, no. 3, pp. 1402–1409, Jul. 2008.

[75] H. Hashemi and D. Tholl, "Analysis of the rms delay spread of indoor radio propagation channel," in *Proceedings of IEEE Int. conference on Commun., ICC'92*, Chicago, USA, pp. 875–881, 14-18, Jun. 1992.

[76] T. S. Rappaport, *Wireless Communications: Principles and Practice.* Prentice-Hall, Inc., 2002.

[77] P. J. Pupalaikis, *The Relationship Between Discrete-Frequency S-parameters and Continuous-Frequency Responses.* DesignCon, http://cdn.teledynelecroy.com/files/whitepapers/designcon2012_lecroy_s-parameters_discrete_frequency_continuous_response.pdf, 2012.